Environmental Earth Sciences (2018) 77:422
https://doi.org/10.1007/s12665-018-7597-x

ORIGINAL ARTICLE

Liquefaction severity mapping based on SPT data: a case study in Canakkale city (NW Turkey)

M. Celal Tunusluoglu[1] · **Oznur Karaca**[1]

Received: 13 October 2017 / Accepted: 5 June 2018 / Published online: 13 June 2018

Abstract

Soil liquefaction is one of the major causes of damage to buildings and structures during earthquakes. Very shallow groundwater table in Quaternary alluvial deposits and the seismic properties of a region can cause a significant damage to buildings and infrastructure dependent on liquefaction. Canakkale city is located in the first-degree seismic hazard zone according to the earthquake zone map of Turkey. A large part of the Canakkale settlement area is located on unconsolidated alluvium recently deposited by the Saricay River. In this survey, the liquefaction potential of the Canakkale settlement area was investigated based on the liquefaction severity index and liquefaction potential index for two possible earthquake scenarios with a moment magnitude (M_w) and peak ground acceleration (a_{max}) of 7.5 and 319 gal and 7.0 and 222 gal, respectively. In addition, these two methods were analysed using the peak ground acceleration (a_{max} = 141 gal) value measured at the Canakkale station during the 2014 Aegean Sea earthquake. Based on the results of the analyses, liquefaction susceptibility maps of Canakkale city were produced for different a_{max} values. The study involved three stages: field work, laboratory testing, and generation of the liquefaction severity maps. Geotechnical boreholes at 151 locations were drilled and Standard Penetration Tests (SPT) performed. Thereafter, natural moisture content, unit weight, grain-size distribution, and Atterberg limits were determined by means of laboratory testing. Finally, Quaternary alluvial deposits in the study area were divided into five classes representing very low-to-very high liquefaction for three a_{max} values.

Keywords Liquefaction · Canakkale · Liquefaction severity index · Liquefaction potential index · Standard penetration test

Introduction

Liquefaction of soil is defined as saturated or partially saturated cohesionless soil deposits substantially losing their strength and stiffness in response to an applied stress, usually earthquake shaking. In this phenomenon, the soil behaves much like a dense, viscous liquid. Liquefaction is one of the most important, interesting, complex, and controversial topics in geotechnical earthquake engineering. In 1964, two major earthquakes that attracted the attention of geotechnical engineers occurred in Niigata (Japan) and Alaska. Both earthquakes induced soil liquefaction producing extensive structural damage and loss of life in urban areas. In the 50 years since these earthquakes, liquefaction has been studied extensively by hundreds of researchers around the world (Kramer 1996).

The liquefaction potential is evaluated by field tests in engineering geology and geotechnical engineering studies. Different types of in situ tests including the standard penetration test (SPT), the cone penetration test (CPT), measurement of in situ shear wave velocity (V_s), and the Becker penetration test (BPT) are used to predict the liquefaction potential of soil (Youd et al. 2001). Among different types of in situ tests, the SPT (ASTM D1586-99 2004) is generally preferred for the evaluation of liquefaction in most countries and is used in this paper. Seed and Idriss (1971) suggested a number of SPT-based simplified methods. This method has been modified and improved for over 45 years by several researchers (e.g., Seed et al. 1985; Youd et al. 2001; Idriss and Boulanger 2004; Cetin et al. 2004).

The study site, at the coordinates between 4,441,000–4,447,000N latitude and 449,000–453,000E longitude (UTM Zone 35N, ED50), covers an area of about 17 km^2 (Fig. 1). Canakkale is one of the important cities in

✉ M. Celal Tunusluoglu
ctonoz@gmail.com

[1] Department of Geological Engineering, Canakkale Onsekiz Mart University, 17020 Canakkale, Turkey

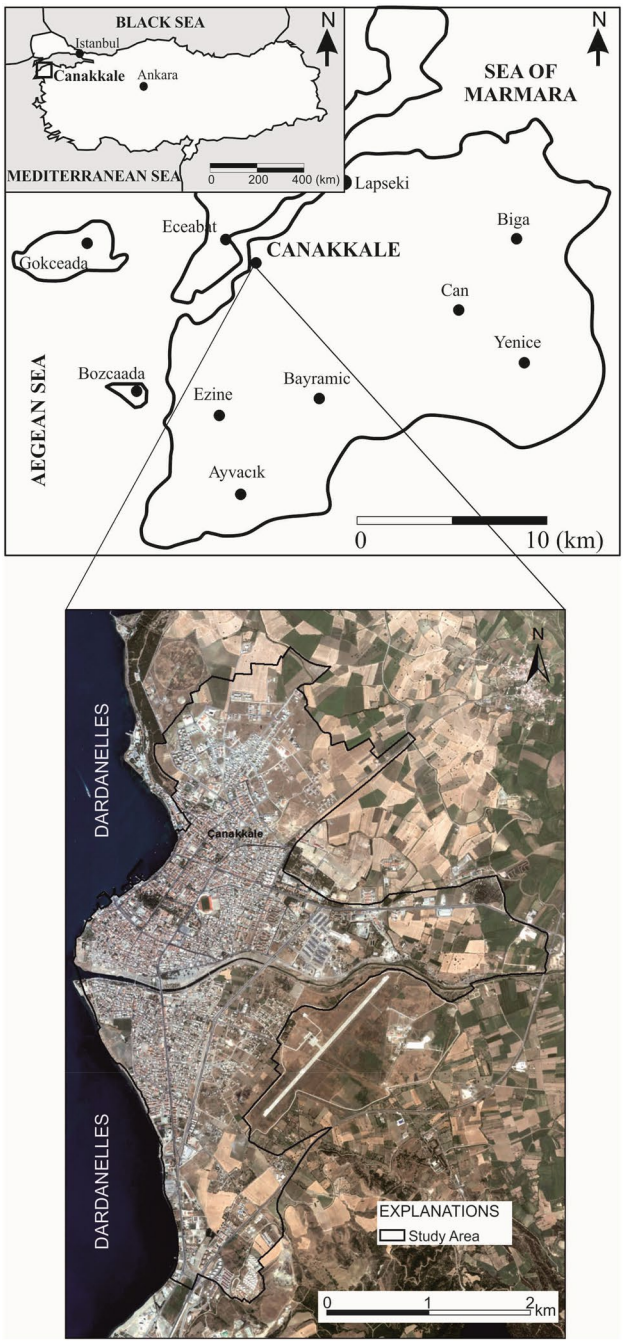

Fig. 1 Location map of the study area

Turkey connecting the two continents (Europe and Asia) and is a developing city. The Canakkale settlement area contains three different soil types. Quaternary alluvial deposits are one of the soil types and are located everywhere in the Canakkale city. Distribution and generation of these alluvial deposits are linked to the impact of the Saricay River which flows through the city from east to west. The groundwater-level variation in alluvium is between 0.6 and 9.9 m below the surface; the mean groundwater depth in the Canakkale city centre is about 2.0 m (Fig. 2). Canakkale city, which is located in the northwestern part of Turkey, is bounded by north and central segments of the North Anatolian Fault Zone (NAFZ) (Yaltırak et al. 2012). The city of Canakkale is situated in a seismically active region according to the earthquake zone map of Turkey produced by the Ministry of Public Works and Settlement, General Directorate of Disaster Affairs (1996).

The main purpose of this paper is to determine the soil vulnerability to liquefaction for different earthquake scenarios and to prepare liquefaction severity maps for the city of Canakkale using the liquefaction severity index (L_S) and liquefaction potential index (LPI). The study involved three stages: field work, laboratory testing, and generation of the liquefaction severity maps. In the first step, geotechnical boreholes were drilled and SPTs were performed, and in addition, disturbed samples were taken using an SPT sampler. In the second step, grain-size distribution was determined by means of laboratory testing. Field-based SPT values were used to calculate the factor of safety against liquefaction (F_L). The F_L of a saturated soil is expressed as the ratio of the cyclic resistance ratio (CRR) to the cyclic stress ratio (CSR). The liquefaction-prone areas in the city of Canakkale were examined based on a simplified procedure by Youd et al. (2001). In addition, the calculation of probability of liquefaction (P_L) and L_S correlations was determined according to a recent method proposed by Sonmez and Gokceoglu (2005). In addition, the LPI modified by Sonmez (2003) was used and compared with the L_S. These methods were applied to determine the liquefaction potential of different areas (Yilmaz and Bagci 2006; Sonmez and Ulusay 2008; Yalcin et al. 2008; Dixit et al. 2012).

Geological setting and seismotectonics of the Gallipoli and Biga Peninsulas

Canakkale settlement area is located in the Canakkale basin which is formed by Middle Miocene-Pliocene sedimentary units ("Canakkale Group", Siyako 2006) and alluvial deposits. The Canakkale Group consists of the Gazhanedere Formation, Kirazli Formation, Camrakdere Formation, and Alcitepe Formation from bottom to top. The Kirazli and Camrakdere Formations are absent in the study area (Fig. 3). The Gazhanedere Formation outcrops in the southeastern part of the study area. It consists of conglomerate, sandstone, and reddish grey mudstone (Atabey et al. 2004).

The Alcitepe Formation outcrops in the northern part of the study area. It generally consists of sandstone, mudstone, sandy, and clayey limestone (Senturk and Karakose 1987). A large part of the Canakkale settlement area is located on alluvial deposits which were formed by the Saricay River.

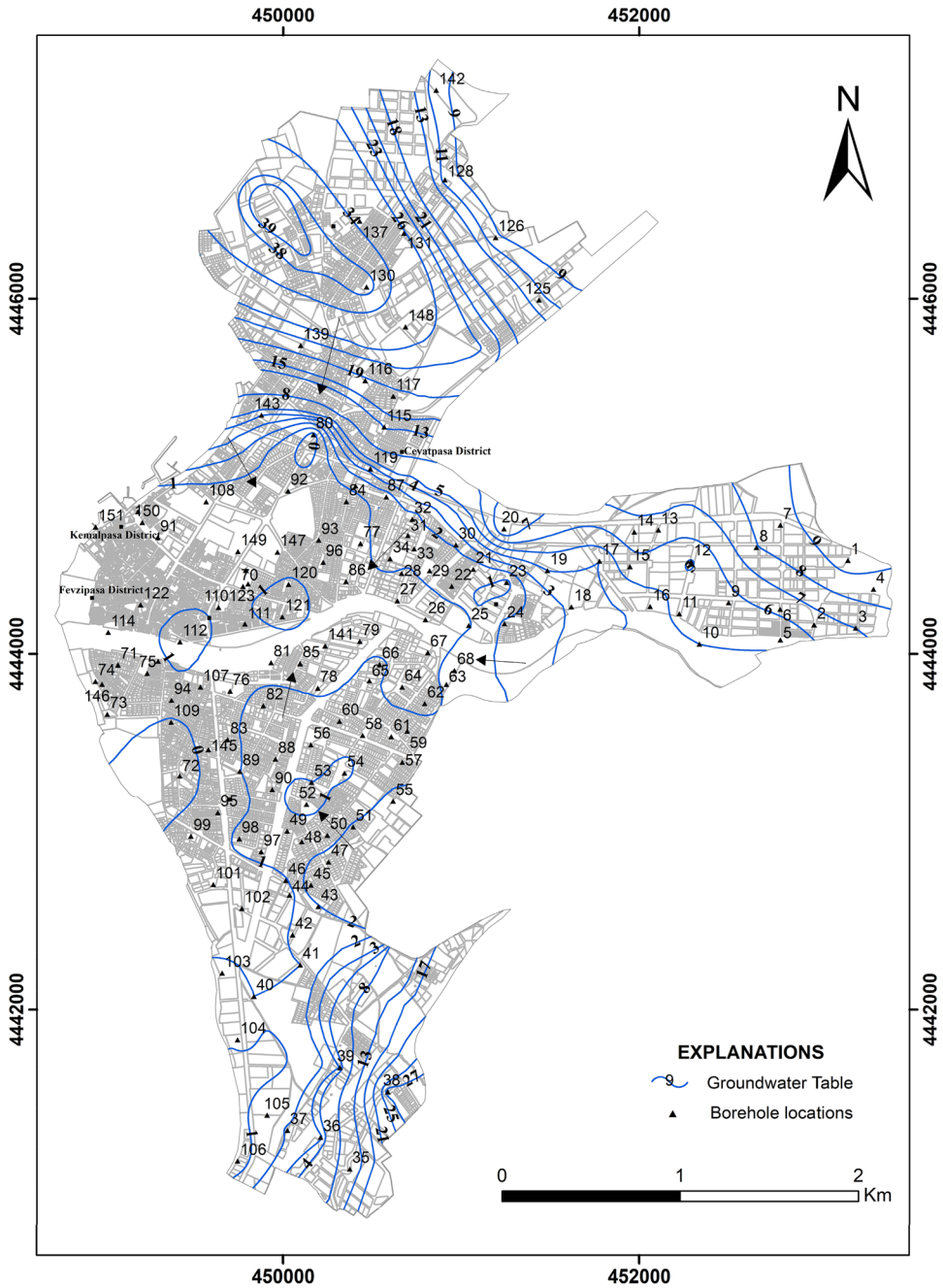

Fig. 2 Groundwater map of the study area

Typical cross sections depicting the subsurface profile of the study area are given in Fig. 4.

Turkey is located in seismically active region of the world. The NAFZ is a 1200 km-long transform fault forming the boundary between the Anatolian and Eurasian plates (Okay et al. 2000). Canakkale, which is situated in the northwest of Turkey, is approximately 40 km southeast of the Saros–Gazikoy segment which is the northern branch of the NAFZ in the Gallipoli peninsula region (Fig. 5). The Saros–Gazikoy segment is locally called the Ganos fault (Rockwell et al. 2001). In 1912, the Ganos fault generated an earthquake with a magnitude (M_s) of 7.3. The central branch of the NAFZ which is located in the Biga peninsula region is composed of many fault zones. The Yenice–Gonen fault is one of these. The southeast of the study area is 70 km from the Yenice–Gonen fault. In 1953, the Yenice–Gonen fault generated the Yenice–Gonen earthquake with a magnitude (M_s) of 7.2. In addition to the faults mentioned, the Edremit fault zone is located farthest from the study area is. It is 75 km from the south of the study area. In 1944, this fault zone produced an earthquake of magnitude (M_s) 6.8 (Fig. 5).

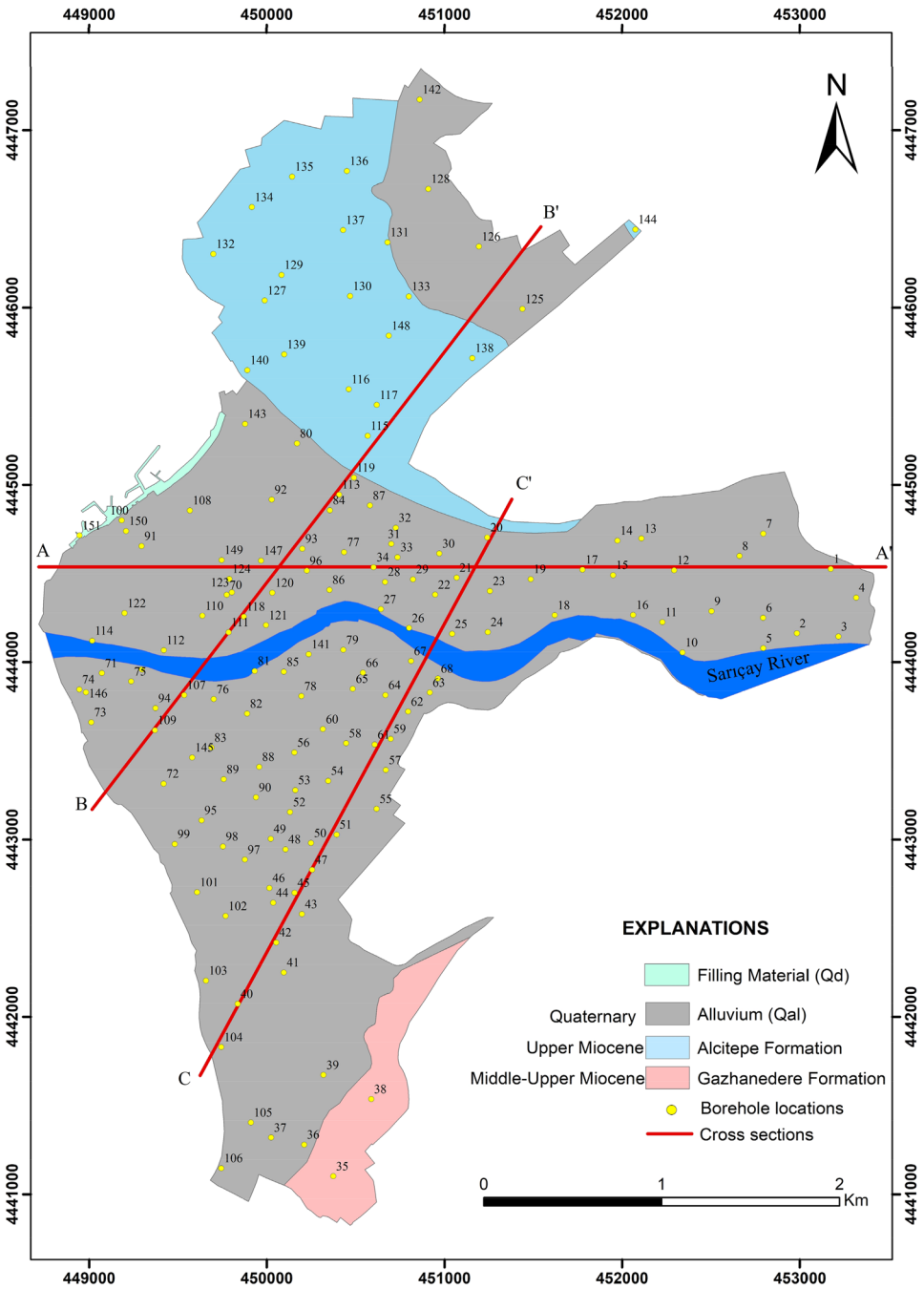

Fig. 3 Geological map of the study area

More recently, the 2014 Aegean Sea earthquake occurred in the northern Aegean Sea on May 24 at 12:25:01 (local time). It had moment magnitude (M_w) of 6.5 and depth of 25.02 km with epicentral coordinates determined as 36.75230 N, 36.03700 E (KOERI 2014; AFAD 2014). The epicentre of the 2014 Aegean Sea earthquake was 93 km away from Canakkale. The peak ground acceleration (a_{max}) recorded was 141 gal (NS component) at the Canakkale station (AFAD 2014). This earthquake was strongly felt in the centre of Canakkale. However, no serious damage and liquefaction phenomena were reported in the city of Canakkale (AFAD 2014; Yildirim et al. 2015).

Determination of peak ground acceleration

Earthquakes with magnitudes of 4.0 and larger ($M_s \geq 4.0$) occurring in the study area and within a radius of 100 km from 1900 to 2018 which were taken from a website based on Disaster and Emergency Management Presidency (AFAD) records are shown in Fig. 6. The equation (Eq. 1)

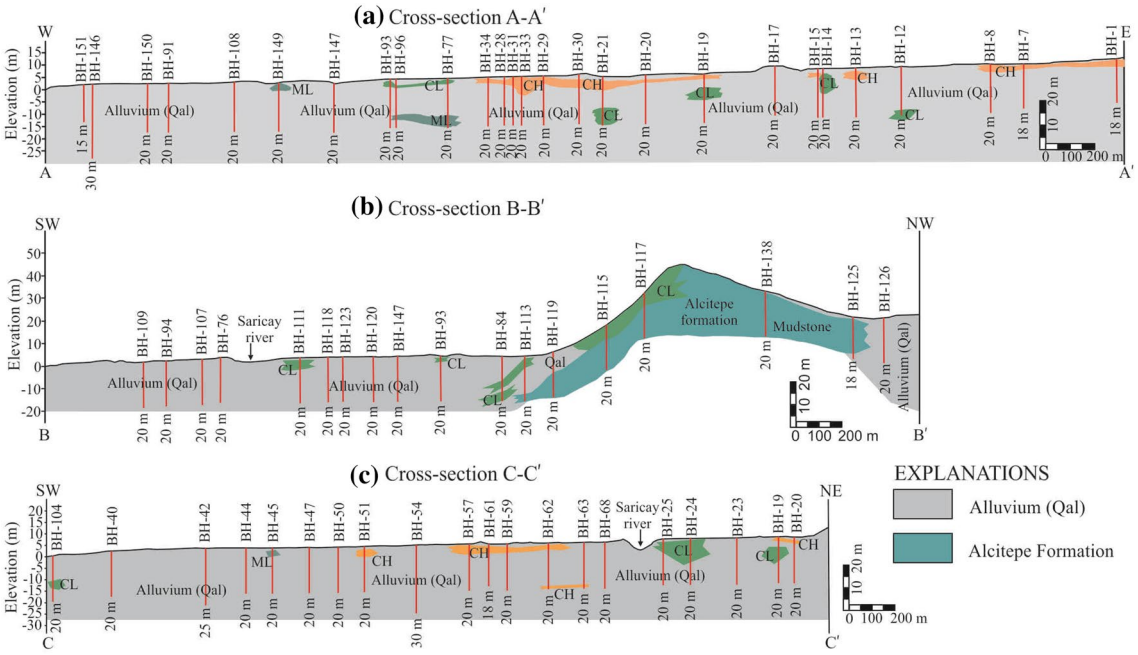

Fig. 4 Engineering geological cross sections for the study area

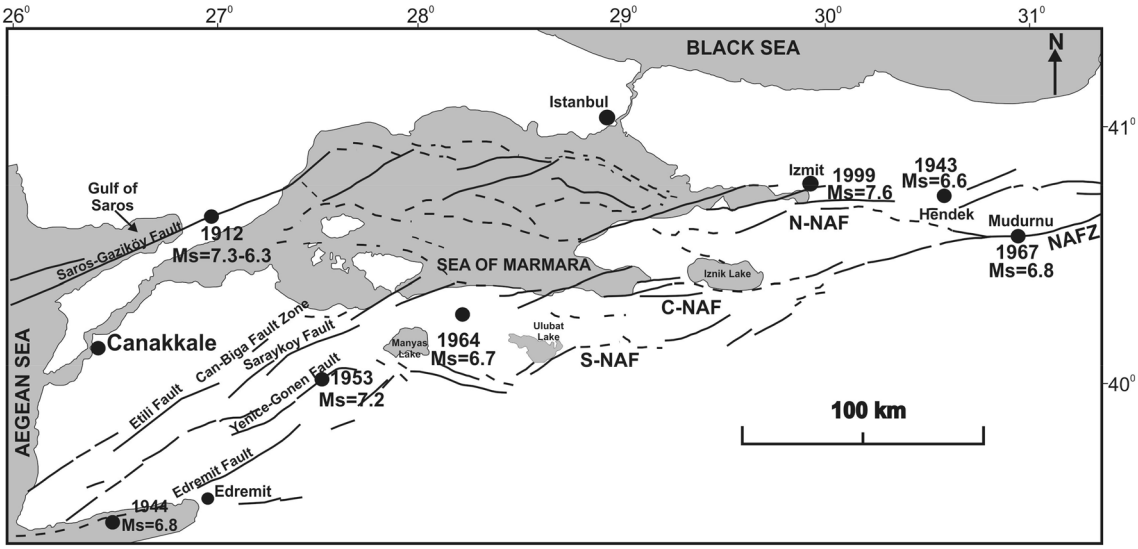

Fig. 5 Active tectonic map of the Marmara region (Gurbuz et al. 2000)

proposed by Well and Coppersmith (1994) can be used to estimate the largest possible earthquake that can be produced by a fault in terms of M_w. In this proposed equation, the surface rupture length (SRL) is used as the input parameter.

$$M_w = 5.08 + 1.16 \times \log(\mathrm{SRL}). \quad (1)$$

In this study, the length of the fault is considered to be more realistic for the prediction of magnitudes, instead of SRL. The fault lengths were taken from the active fault map of Turkey produced by the General Directorate of Mineral Research and Exploration (MTA) (2012). In Table 1, the three major faults located within a radius of 100 km from the centre of the study area are considered (Tunusluoglu 2014). Based on this information, the seismicity of the study area is considered to be quite high. In liquefaction assessment methods, the triggering effect of an earthquake on liquefaction should be taken into consideration as a_{max} produced by the earthquake. The a_{max} considered for liquefaction assessment

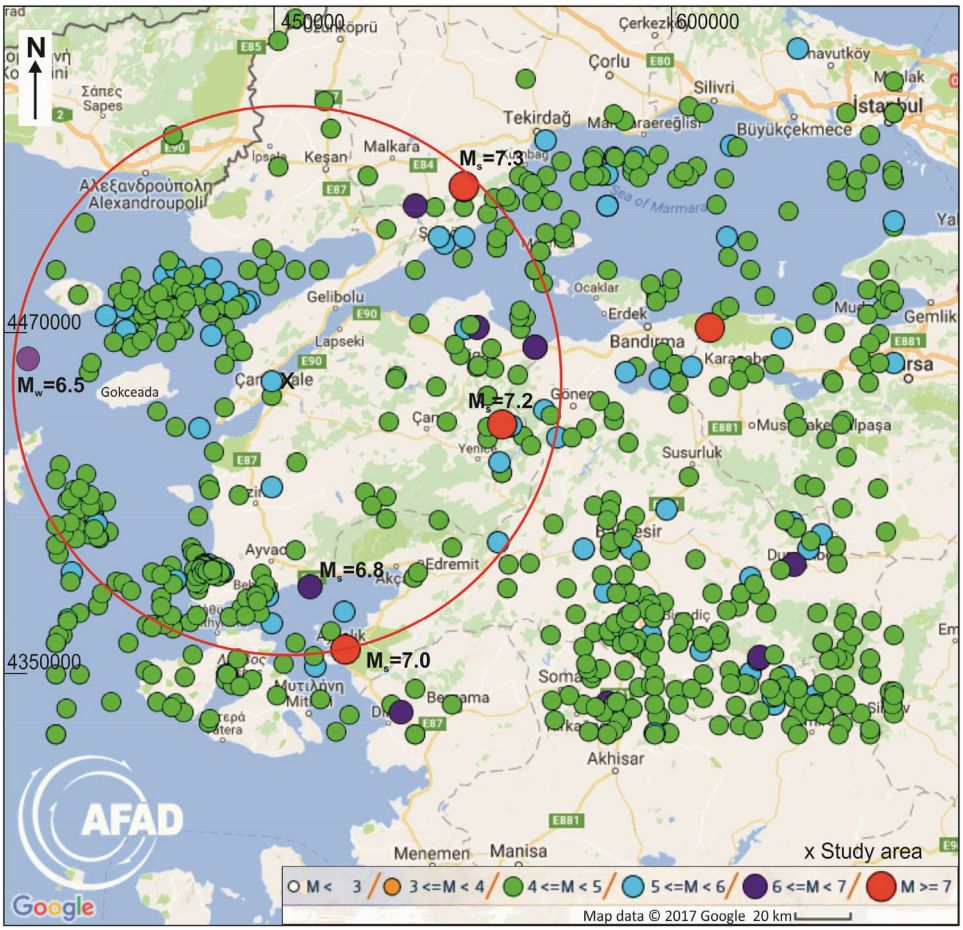

Fig. 6 Distribution of earthquakes ($M_s \geq 4.0$) in the study area and its surroundings (http://www.deprem.gov.tr/en/eventcatalogue)

Table 1 Important faults belonging to the study area and its surroundings, and the largest earthquake moment magnitudes produced by these faults (Tunusluoglu 2014)

Fault	SRL (km)	M_w
Saros–Gazikoy fault	125	7.5
Yenice–Gonen fault	70	7.2
Edremit fault	125	7.5

SRL surface rupture length

Table 2 Peak ground accelerations to be produced by faults located in the study area and its surroundings

Fault	M_w	The nearest distance of the fault to the study area, Re (km)	a_{max} (gal)
Saros–Gazikoy fault	7.5	40	319
Saros–Gazikoy fault	7.0	40	222
Yenice–Gonen fault	7.2	70	133
Edremit fault	7.5	75	149

in the study area was evaluated with the attenuation equation proposed by Ulusay et al. (2004). This relationship is based on the large Turkish earthquake database and considers different ground conditions:

$$a_{max} = 2.18\, e^{0.0218\,(33.3M_w - \mathrm{Re} + 7.8427\,S_A + 18.9282S_B)}, \quad (2)$$

where $S_A = 0$, $S_B = 0$ (rock), $S_A = 1$, $S_B = 0$ (soil), and $S_A = 0$, $S_B = 1$ (loose soil).

A large part of the investigated area is composed of alluvium. For this reason, when taking $S_A = 0$, $S_B = 1$, the closest distance of each fault to the investigation area was considered to be Re. The largest horizontal ground acceleration values which can be produced by the three major faults were calculated using the attenuation equation (Eq. 2), and the results are given in Table 2. As seen from Table 2, the a_{max} that can be produced by an earthquake of 7.5 moment magnitude in the Saroz–Gazikoy Fault Zone was calculated as 319 gal. In addition, a second possible earthquake scenario was considered at a magnitude (M_w) of 7.0 along the Saroz–Gazikoy Fault Zone. The a_{max} was calculated as approximately 222 gal for the Saroz–Gazikoy Fault Zone (Table 2).

The 2014 Aegean Sea earthquake was recorded by three accelerometer stations in Canakkale city (AFAD 2014). The a_{max} recorded was 141 gal (NS component) at the Canakkale centre station. In addition, using the Aegean Sea earthquake data, the a_{max} value was calculated using the attenuation equation proposed by Ulusay et al. (2004). The calculated peak ground acceleration (a_{max} = 46.5 gal) value is close to the values measured at Canakkale-Kepez station (a_{max} = 45.3 gal NS component and 51.1 gal EW component). However, the peak ground acceleration (a_{max} = 141 gal) value was used in this study.

Field studies and geotechnical evaluation

151 geotechnical boreholes were opened with a total depth of 3000 m to obtain disturbed and undisturbed soil samples, to implement the SPT, and to determine the static water level from the ground surface (Buyuksarac et al. 2013). The depth of the groundwater level varies between 0.6 and 17.1 m depth. In addition, groundwater depth was mapped (Fig. 2). During the 2 years of measurements, the variation in groundwater levels was determined to be between 0.1 and 3.5 m (Deniz 2005). The depths of 140 boreholes were 20 m and the depths of other boreholes range between 15 and 30 m. During the field studies, SPTs (ASTM D1586-99 2004) were conducted at every 1.5 m depth. The Canakkale settlement area comprises three different units. The Alcitepe and Gazhanedere Formations are described as rock materials. Quaternary alluvial deposits are located at the centre, the eastern, the northern, and the southern parts of Canakkale city (Fig. 3). 131 geotechnical boreholes were drilled in alluvial deposit areas. As shown in Fig. 4, most of the areas in the investigated region are alluvium. Sandy areas (SP, SW, SC, and SM) are shown as alluvium in general and clays are shown separately. In some places in the alluvial deposits, the SPT-N values are 10 at the ground surface with a depth of 5 m. At the lower strata, the SPT-N increases, but the density of the soils at these depths can be described as loose-to-moderately dense. In addition, at depths between 10 and 20 m, the average value of SPT-N counts varies between 10 and 25 (Fig. 7). However, in some locations in the alluvial deposits, drill rods were swamped by weight in the borehole at depths between 4.5 and 12 m.

Laboratory tests were undertaken on undisturbed and disturbed soil samples taken by Shelby tube and SPT sampler from the 151 boreholes, to determine the index properties of the soil samples. They included natural moisture content,

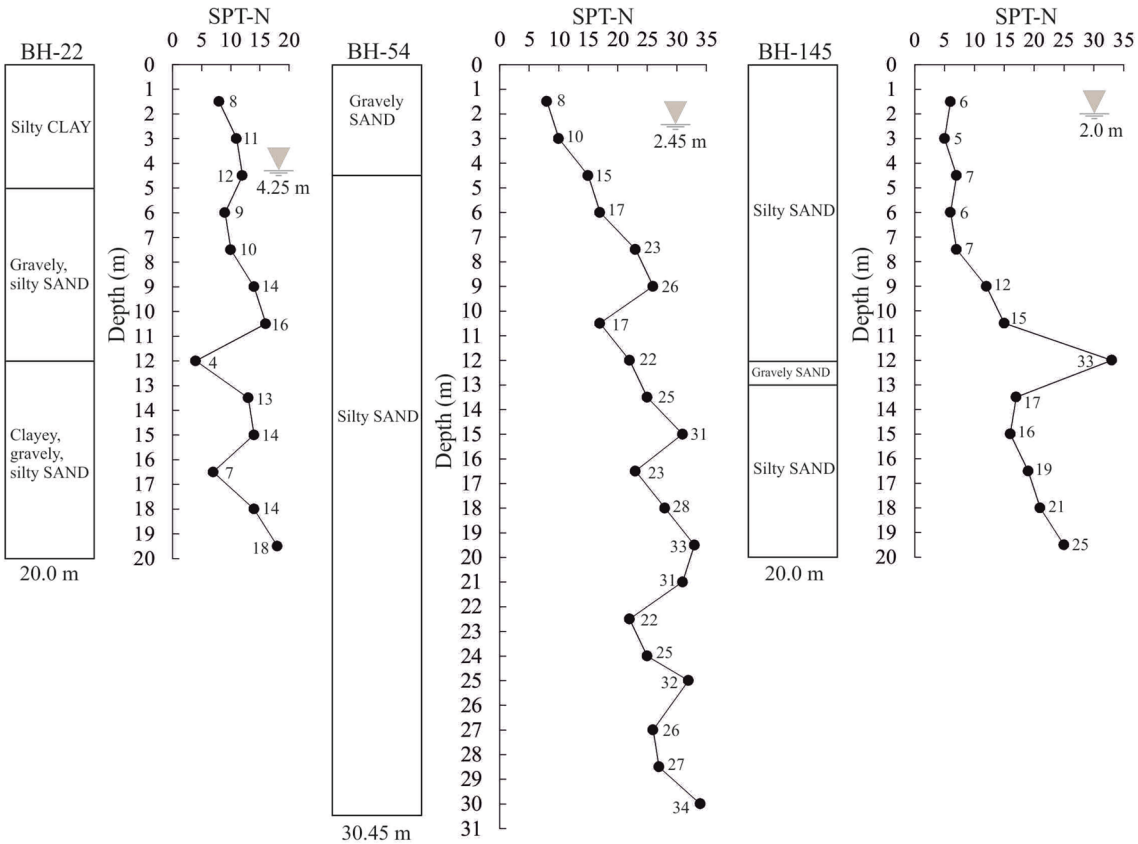

Fig. 7 Selected engineering logs illustrating the SPT-N values and groundwater conditions in the study area

unit weight, grain-size distribution (sieve and hydrometer methods), and Atterberg limits. The laboratory tests were carried out following the procedures described by ASTM (2004). The study area is formed by alluvium with fine-grained soils in the upper levels and coarse-grained soils in the lower levels. Unit weight was determined from the undisturbed samples which were taken at the depth of 2.5–3.0 m. Unit weight values vary between 18.1 and 18.4 kN/m^3. Natural moisture contents of the fine-grained soils varied between 7.3 and 67.6%. The fine-grained soils in the study area are formed, on average, of 1.4% gravel, 20.8% sand, and 77.8% fines (silt–clay). The liquid limit of the fine-grained soils changes between 24.0 and 73.5%. The plasticity index values vary between 7.0 and 44.0%. Coarse-grained soils are comprised of sand and form the bottom layer of alluvium. Natural moisture contents of the coarse-grained soils varied between 4.3 and 61.5%. The coarse-grained soils in the study area consist of, on average, of 3.0% gravel, 85.1% sand, and 11.9% fines (silt–clay). The liquid limit of the coarse-grained soils changes between 23.5 and 56.5%. The plasticity index values range between 5.9 and 27.2% (Table 3).

The Unified Soil Classification System (USCS) was used to describe the soils which were taken from boreholes. Based on the results of the grain-size analysis, 80% of the samples are coarse-grained and 20% of the samples are fine-grained soils. The fine-grained fraction mostly consists of low plasticity clay of classification CL (10.1%) and CH (8.1%), and in a few locations, inorganic silt of classification, ML, MH, and CL–ML were also encountered. All the coarse-grained soils in the study area consist of sand and 25% of them are SM (silty sand) according to USCS. Figure 8 shows the upper and lower limits in the gradation curves for liquefiable and potentially liquefiable soils and the position of grain-size distribution of the soils collected from different depths by SPT tubes. It was seen that the obtained grain-size distribution curves fell within the range of liquefiable soils as specified by the Japanese Port and Harbor Research Institute (JPHRI 1989 from Lee et al. 2004).

Table 3 Geotechnical properties of the Quaternary alluvium at the centre, the eastern, the northern, and the southern of Canakkale city

Property	Fine-grained soils (ML, CL, MH, and CH)						Coarse-grained soils (SC, SM, SP, and SW)					
	Sample count	Min	Max	Mean	SD	SE	Sample count	Min	Max	Mean	SD	SE
Nat. water cont., w_n (%)	208	7.3	67.6	27.6	8.64	0.60	–	–	–	–	–	–
Unit weight γ_n, (kN/m^3)	29	18.13	18.39	18.27	0.08	0.02	–	–	–	–	–	–
Liquid limit LL (%)	163	24	73.5	47.6	11.86	0.93	36	23.5	56.5	32.4	6.05	1.01
Plastic limit P_L (%)	163	13	55.2	23.5	5.11	0.40	36	14.3	29.3	17.6	3.30	0.55
Plasticity index PI (%)	163	7	44	22.4	8.27	0.65	36	5.9	27.2	14.8	3.79	0.63
# 4 sieve (%)	208	0	8.1	1.4	1.55	0.11	819	0	43.6	3	5.89	0.21
# 200 sieve (%)	208	51.2	96.8	77.8	11.37	0.79	819	0.2	83	11.9	9.75	0.34

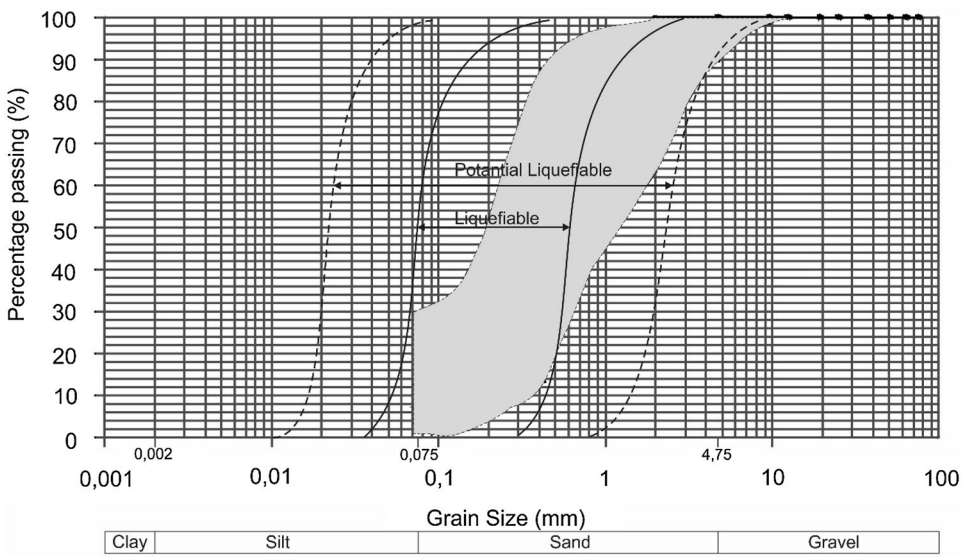

Fig. 8 Grain-size distribution of the soils

Liquefaction assessment

The liquefaction potential of an area can be evaluated by laboratory tests or in situ tests and empirical methods. Due to the difficulties associated with obtaining good soil samples, empirical approaches based on the in situ penetration test methods are widely used. Among different types of in situ tests, the SPT is generally preferred for evaluating liquefaction potential in most countries (Chu et al. 2004; Vipin et al. 2010; Dixit et al. 2012; Sharma and Hazarika 2013; Kang et al. 2014; Rahman et al. 2014) and in Turkey (Ulusay et al. 2000, 2007; Ulusay and Kuru 2004; Yilmaz and Yavuzer 2005; Yilmaz and Bagci 2006; Hasancebi and Ulusay 2006; Yalcin et al. 2008; Sonmez and Ulusay 2008; Sonmez et al. 2008; Ulamis and Kilic 2008; Tosun et al. 2011; Akin et al. 2013; Duman et al. 2015). The liquefaction potential in this study was investigated by the simplified SPT-based method proposed by Seed and Idriss (1971) and Seed et al. (1985). It also considered the modifications suggested by Youd et al. (2001). In this study, corrected SPT-N values were used using the equation suggested by Liao and Whitman (1986). Seed and Idriss (1971) proposed the cyclic stress ratio (CSR) which is defined as cyclic shear stress required to cause liquefaction. Youd et al. (2001) proposed a slight modification in the calculation of CSR. Seed et al. (1985) presented an empirical correlation which is determined from the correlation between corrected SPT $(N_1)_{60}$ and the CSR. The empirical correlation curves, which are the same as the liquefaction triggering curves, represent the capacity of the soil to resist liquefaction referred to as the cyclic resistance ratio (CRR). Youd et al. (2001) modified the CRR curves from Seed et al. (1985). This CRR modification is comprised of clean sands and magnitude 7.5 earthquakes. CRR curves represent limiting conditions that determine whether liquefaction will occur for a magnitude of 7.5. In addition, CRR curves were developed for granular soils with the fines contents of 5% or less, 15, and 35% (Youd et al. 2001). In this study, the CRR equation proposed by Youd et al. (2001) was taken into consideration. To assess the liquefaction analyses, the equation for factor of safety (FS) against liquefaction is written in terms of CRR7.5, CSR, and MSF as follows (Eq. 3):

$$\mathrm{FS} = \left(\mathrm{CRR}_{7.5}/\mathrm{CSR}\right)\mathrm{MSF}. \tag{3}$$

The magnitude scaling factor (MSF) in Eq. 4 was employed in this study (Youd et al. 2001):

$$\mathrm{MSF} = \frac{10^{2.24}}{M_{\mathrm{w}}^{2.56}}. \tag{4}$$

In this study, the distributions of the corrected SPT $(N_1)_{60}$ data versus the CSR data are compared with the CRR curves modified by Youd et al. (2001) (Fig. 9). This comparison was made for two different $a_{\max}$. In Fig. 9, 100 of 131 borehole data have high and very high liquefaction intensity indices for 319 gal. These borehole data fall to the left of the curve (FC = 15%) and 8 borehole data are located between the two curves (FC = 35% and FC = 15%). For 222 gal, 34 borehole data from 131 borehole data have high and very high liquefaction intensity indices. Twenty-one borehole data fall to the left of the curve (FC = 35%) and 3 borehole data are located between the two curves (FC = 15% and FC = 5%).

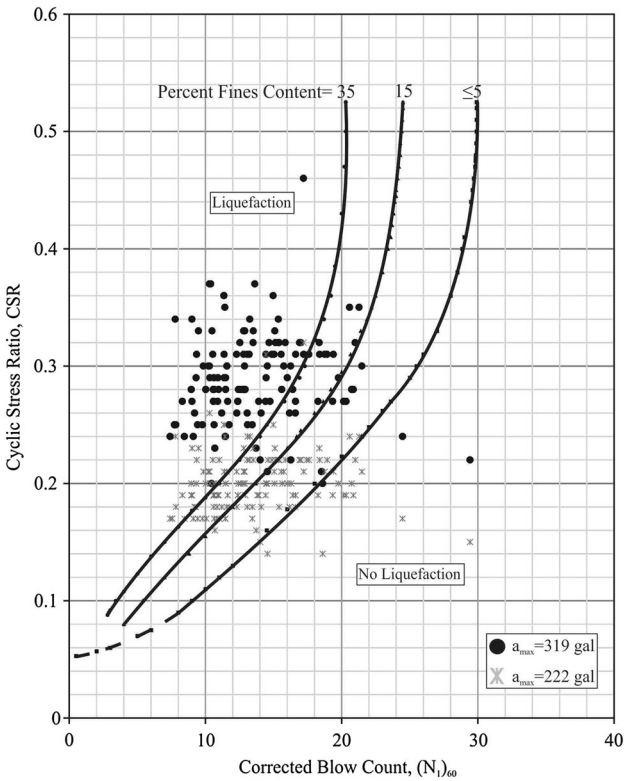

Fig. 9 Cyclic stress ratio and SPT $(N_1)_{60}$ plot based on Youd et al. (2001)

In addition, the hydrometer and the Atterberg limits experiments were carried out on 177 soil samples taken from different depths of 73 boreholes in alluvial deposit areas. Fifty-two samples from a total of 177 samples are composed of silty clay (CL = 48 unit), silty sand (ML = 3 unit) and silty clay–silty sand (CL-ML = 1 unit) soils. The liquefiability of these soils was also investigated using the method proposed by Seed et al. (2003) (Fig. 10). Six samples falling into the A region and 46 samples falling into the B region were defined using this method (Fig. 10). According to the procedure of Seed et al. (2003), 6 samples falling into zone A and 34 samples falling into zone B were defined as liquefiable.

In the literature, the liquefaction potential of the loose sand layers which are susceptible to liquefaction up to a depth of 20 m from the surface is assessed (Seed and Idriss 1971; Sonmez 2003). Studies indicate that the liquefaction

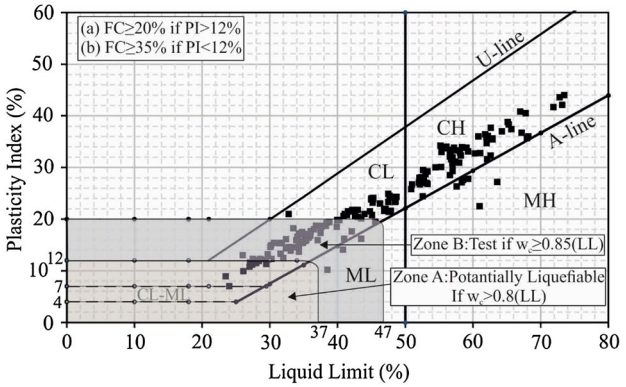

Fig. 10 Liquefaction potential of silty soils (Seed et al. 2003)

phenomenon occurs when the factor of safety is less than 1.0. In addition, it is stated that the liquefaction phenomenon is defined as marginally liquefiable with the factor of safety ranging between 1.0 and 1.2, but the liquefaction phenomenon will not occur above 1.2 (Tosun and Ulusay 1997; Ulusay and Kuru 2004; Duman et al. 2015). However, Seed and Idriss (1982) indicated that the admissible factor of safety value for the liquefaction phenomenon is between 1.25 and 1.5.

Iwasaki et al. (1982) proposed a liquefaction potential index (LPI) to remove the limitations of the factor of safety (F_L). LPI was defined in four categories of liquefaction potential (very low, low, high, and very high). The LPI is calculated by the following equations (Eqs. 5a, 5b, 5c, 5d, 5e):

$$\mathrm{LPI} = \int_0^{20} F(z)W(z)\mathrm{d}z, \tag{5a}$$

$$F(z) = 1 - F_L \quad \text{for } F_L < 1.0, \tag{5b}$$

$$F(z) = 0 \quad \text{for } F_L \geqslant 1.0, \tag{5c}$$

$$W(z) = 10 - 0.5z \quad z < 20\ \mathrm{m}, \tag{5d}$$

$$W(z) = 0 \quad z \geqslant 20\ \mathrm{m}, \tag{5e}$$

where z is the depth of the midpoint of the soil layer in metres and F_L is the factor of safety against liquefaction. Boundary values of LPI are given in Table 4 with liquefaction susceptibility descriptions.

However, this classification has some limitations. These limitations which are "non-liquefiable" and "moderate" liquefaction potential categories are not defined in the LPI. Therefore, Sonmez (2003) modified the classification by including these two categories in the classification (Table 5). In addition, Sonmez (2003) modified the

Table 4 Liquefaction potential classification suggested by Iwasaki et al. (1982)

Liquefaction index (LPI)	Description
0	Very low
$0 < \mathrm{LPI} \leq 5$	Low
$5 < \mathrm{LPI} \leq 15$	High
$15 > \mathrm{LPI}$	Very high

$F(z)$ term. $F(z)$ is expressed by the following equations (Eqs. 6a, 6b, 6c):

$$F(z) = 0 \quad \text{for } F_L \geqslant 1.2, \tag{6a}$$

$$F(z) = 2 \times 10^6 \mathrm{e}^{-18.427F_L} \quad \text{for } 1.2 > F_L < 0.95, \tag{6b}$$

$$F(z) = 1 - F_L \quad \text{for } F_L < 0.95. \tag{6c}$$

The $F_L = 1.2$ threshold value used in this modification is considered to be the lowest value at which liquefaction does not occur. However, Sonmez (2003) stated that the threshold value of $F_L = 1.2$ from marginally liquefiable to non-liquefiable could change according to the results of future studies.

The probability of soil liquefaction (P_L) depends on the value of F_L suggested by Juang et al. (2003). Sonmez and Gokceoglu (2005) proposed the liquefaction severity index (L_S) and the authors also preferred to use P_L in this index equation. It is stated by Sonmez and Gokceoglu (2005) that the use of the liquefaction probability equation in the concept of liquefaction index will be more consistent. The L_S is calculated by the following equations (Eqs. 7a, 7b, 7c, 7d, 7e):

$$L_S = \int_0^{20} P_L(z)W(z)\mathrm{d}z \tag{7a}$$

$$P_L = \frac{1}{1 + (F_L/0.96)^{4.5}} \quad \text{for } F_L \leqslant 1.411, \tag{7b}$$

$$P_L(z) = 0 \quad \text{for } F_L > 1.411, \tag{7c}$$

$$W(z) = 10 - 0.5z \quad z < 20\ \mathrm{m} \tag{7d}$$

$$W(z) = 0 \quad z \geqslant 20\ \mathrm{m}, \tag{7e}$$

Table 5 Liquefaction potential classification suggested by Sonmez (2003)

Liquefaction index (LPI)	Description
0	Non-liquefied (based on $F_L \geq 1.2$)
$0 < \mathrm{LPI} \leq 2$	Low
$2 < \mathrm{LPI} \leq 5$	Moderate
$5 < \mathrm{LPI} \leq 15$	High
15 >	Very high

where z is the depth of the midpoint of the soil layer in metres and F_L is the factor of safety against liquefaction. Boundary values of L_S are given in Table 6 with liquefaction susceptibility descriptions.

Liquefaction severity map of Canakkale settlement area

Preparation of the liquefaction severity maps is a valuable solution to evaluate the effects of soil liquefaction in urban planning and earthquake-resistant design of constructions. In this study, the liquefaction potential of the Canakkale settlement area was investigated based on the liquefaction severity index and liquefaction potential index using the methods proposed by Sonmez and Gokceoglu (2005) and Sonmez (2003), respectively. Two possible earthquake scenarios with an M_w and a_{max} of 7.5 and 319 gal and 7.0 and 222 gal, respectively, were considered. Furthermore, these two methods were analysed using the a_{max} value measured at the Canakkale station during the 2014 Aegean Sea earthquake. According to both liquefaction methods, for the a_{max} of 141 gal, liquefaction analyses were also performed. All liquefaction analyses were carried out for 131 boreholes (Tables 7, 8, 9). The liquefaction analysis results obtained for the three different a_{max} values are shown in the pie charts (Fig. 11). According to liquefaction severity index and liquefaction potential index analyses, for $a_{max} = 319$ gal, the Canakkale settlement area is in the categories of high severity (60%) and very high potential (91%), respectively. Moderate areas comprise 16% severity and 1% potential, respectively. For $a_{max} = 222$ gal, the Canakkale settlement area is in the categories of moderate severity (62%) and very high potential (59%), respectively. High areas comprise 21% severity and 30% potential, respectively. For $a_{max} = 141$ gal, the Canakkale settlement area is in the categories of moderate (33%) severity and high (36%) potential, respectively. Low areas are 47% severity and 25% potential, respectively. However, no liquefaction phenomena were reported after the 2014 Aegean Sea earthquake (AFAD 2014; Yildirim et al. 2015). For this reason, it is seen that the liquefaction severity index method is more consistent when the two methods are compared. The liquefaction severity and liquefaction potential index maps of the Canakkale settlement area were created by means of geographic information systems (GIS) software (Figs. 12, 13, 14, 15, 16, 17). As shown in Figs. 12, 13, 14, 15, 16, and 17, the Alcitepe and Gazhanedere Formations are described as non-liquefiable soil ($L_S = 0$) in the study area. Quaternary alluvial deposits in the study area were divided into five classes from very low to very high liquefaction.

Table 6 Liquefaction severity classification suggested by Sonmez and Gokceoglu (2005)

Liquefaction severity (L_S)	Description
$85 \le L_S < 100$	Very high
$65 \le L_S < 85$	High
$35 \le L_S < 65$	Moderate
$15 \le L_S < 35$	Low
$0 < L_S < 15$	Very low
$L_S = 0$	Non-liquefiable

In Turkey, earthquake–soil–building interaction and the importance of liquefaction were proven after the 1998 Ceyhan-Adana and 1999 İzmit earthquakes. Afterwards, Turkish earthquake codes were published in different years. Unfortunately, many buildings were built before these codes without taking necessary precautions. The province of Canakkale is also located in a seismically active region. The population of the Canakkale settlement area has increased in the last 2 decades. Especially after establishment of the university in 1992, the city started to develop and housing demands increased. When we look at the residential areas in Fig. 12, it is seen that almost the entire city area is open for settlement. Although not all of these areas have been constructed, these areas are open for construction and housing will be built in the future. Residential areas in Canakkale were assessed and classified according to their physical vulnerability to natural hazards (earthquakes, landslides, and stream floods) by Basaran et al. (2014). In this study, the building density areas and few-multi storey housing areas were evaluated in five categories. In the study by Basaran et al. (2014), semi-organized and medium density housing developed to the south of Sarıcay River, and organized, multistorey housing remained to the north of Sarıcay River. In addition, housing areas in Canakkale were grouped into four risk zones according to their physical vulnerability to natural hazards by Basaran et al. (2014). It is clear that the liquefaction maps produced in this study match the high-risk zones map of Basaran et al. (2014). As a result, when we overlay the liquefaction map and development plan, it is obvious that some areas may be affected negatively by a possible earthquake. Therefore, understanding the ground conditions and construction of buildings in accordance with earthquake regulations may reduce structural damage.

Conclusion

In this study, geological and geotechnical investigations were carried out in the Canakkale settlement area and the liquefaction severity of the Quaternary alluvial deposits was determined using the methods of liquefaction severity index and liquefaction potential index using two probable earthquake scenarios. In addition, the peak ground acceleration

Table 7 Liquefaction severity index (L_S) and liquefaction potential index (LPI) values for a_{max} = 319 gal (Fm: formation, Qal: alluvium, Tmal: alcitepe Fm, and Tmg: gazhanedere Fm)

Borehole no.	Coordinates		Depth of GWT (m)	L_S	Description	LPI	Description	Fm
	N	E						
1	453,172	4,444,526	3.50	27	Low	15.8	Very high	Qal
2	452,983	4,444,163	6.10	61	Moderate	46.0	Very high	Qal
3	453,215	4,444,145	4.00	63	Moderate	37.8	Very high	Qal
4	453,315	4,444,364	4.70	15	Low	4.50	Moderate	Qal
5	452,794	4,444,079	6.00	55	Moderate	21.0	Very high	Qal
6	452,793	4,444,251	6.00	46	Moderate	19.8	Very high	Qal
7	452,794	4,444,725	3.50	72	High	24.8	Very high	Qal
8	452,660	4,444,599	2.10	82	High	35.2	Very high	Qal
9	452,503	4,444,288	5.50	85	Very high	45.8	Very high	Qal
10	452,339	4,444,055	2.60	80	High	43.9	Very high	Qal
11	452,226	4,444,226	3.65	77	High	34.8	Very high	Qal
12	452,292	4,444,519	4.00	88	Very high	54.6	Very high	Qal
13	452,108	4,444,698	1.80	80	High	42.8	Very high	Qal
14	451,973	4,444,686	2.30	79	High	39.0	Very high	Qal
15	451,949	4,444,491	3.80	90	Very high	44.0	Very high	Qal
16	452,062	4,444,267	4.40	96	Very high	45.9	Very high	Qal
17	451,777	4,444,522	5.30	85	Very high	48.3	Very high	Qal
18	451,620	4,444,265	4.40	86	Very high	34.4	Very high	Qal
19	451,485	4,444,469	2.50	85	Very high	49.7	Very high	Qal
20	451,241	4,444,704	5.20	75	High	29.8	Very high	Qal
21	451,068	4,444,477	4.55	88	Very high	29.0	Very high	Qal
22	450,947	4,444,381	4.25	65	High	41.7	Very high	Qal
23	451,256	4,444,402	5.35	87	Very high	25.4	Very high	Qal
24	451,244	4,444,170	5.10	91	Very high	32.7	Very high	Qal
25	451,043	4,444,160	5.10	85	Very high	42.3	Very high	Qal
26	450,800	4,444,193	5.10	85	Very high	42.3	Very high	Qal
27	450,642	4,444,299	5.30	79	High	36.8	Very high	Qal
28	450,665	4,444,453	4.50	85	Very high	44.4	Very high	Qal
29	450,823	4,444,468	3.60	85	Very high	36.5	Very high	Qal
30	450,971	4,444,613	2.90	80	High	43.4	Very high	Qal
31	450,701	4,444,667	3.55	55	Moderate	10.0	High	Qal
32	450,726	4,444,758	2.60	49	Moderate	11.5	High	Qal
33	450,736	4,444,592	3.70	80	High	49.3	Very high	Qal
34	450,601	4,444,536	3.50	34	Low	20.3	Very high	Qal
35	450,374	4,441,102	1.10	0	Non-liquefiable	0	Non-liquefiable	Tmg
36	450,210	4,441,280	5.25	43	Moderate	1.0	Low	Qal
37	450,024	4,441,320	3.10	60	Moderate	30.7	Very high	Qal
38	450,588	4,441,537	4.00	0	Non-liquefiable	0	Non-liquefiable	Tmg
39	450,319	4,441,673	7.00	36	Moderate	15.8	Very high	Qal
40	449,836	4,442,074	2.00	69	High	33.7	Very high	Qal
41	450,096	4,442,251	3.00	65	High	29.4	Very high	Qal
42	450,053	4,442,420	2.90	82	High	38.5	Very high	Qal
43	450,198	4,442,580	0.65	81	High	44.0	Very high	Qal
44	450,036	4,442,644	2.55	84	High	39.3	Very high	Qal
45	450,156	4,442,700	1.40	80	High	58.1	Very high	Qal
46	450,015	4,442,727	2.10	66	High	23.1	Very high	Qal
47	450,255	4,442,830	1.90	71	High	38.2	Very high	Qal
48	450,105	4,442,945	2.00	74	High	40.5	Very high	Qal
49	450,022	4,443,004	2.00	66	High	27.6	Very high	Qal

Table 7 (continued)

Borehole no.	Coordinates		Depth of GWT (m)	L_S	Description	LPI	Description	Fm
	N	E						
50	450,249	4,442,981	2.20	76	High	46.0	Very high	Qal
51	450,393	4,443,028	1.90	66	High	27.3	Very high	Qal
52	450,131	4,443,155	2.35	66	High	32.7	Very high	Qal
53	450,160	4,443,279	2.40	80	High	40.0	Very high	Qal
54	450,345	4,443,331	2.45	73	High	37.5	Very high	Qal
55	450,618	4,443,173	2.75	93	Very high	48.0	Very high	Qal
56	450,155	4,443,491	2.20	93	Very high	48.0	Very high	Qal
57	450,670	4,443,392	3.30	91	Very high	51.4	Very high	Qal
58	450,446	4,443,543	4.00	93	Very high	50.3	Very high	Qal
59	450,697	4,443,568	3.15	70	High	39.2	Very high	Qal
60	450,316	4,443,623	3.00	85	Very high	36.6	Very high	Qal
61	450,607	4,443,536	3.40	92	Very high	51.4	Very high	Qal
62	450,795	4,443,722	4.50	77	High	35.0	Very high	Qal
63	450,917	4,443,830	2.55	42	Moderate	16.3	Very high	Qal
64	450,668	4,443,815	4.45	80	High	39.5	Very high	Qal
65	450,484	4,443,850	3.90	88	Very high	42.0	Very high	Qal
66	450,541	4,443,941	3.80	74	High	26.8	Very high	Qal
67	450,812	4,444,007	4.60	83	High	35.6	Very high	Qal
68	450,963	4,443,908	3.55	22	Low	0	Non-liquefiable	Qal
69	449,297	4,443,959	1.55	48	Moderate	18.3	Very high	Qal
70	449,774	4,444,380	3.50	69	High	30.5	Very high	Qal
71	449,072	4,443,939	1.40	72	High	23.9	Very high	Qal
72	449,419	4,443,315	2.40	77	High	48.4	Very high	Qal
73	449,012	4,443,662	1.10	73	High	26.5	Very high	Qal
74	448,945	4,443,847	0.80	65	High	26.3	Very high	Qal
75	449,236	4,443,892	1.95	62	Moderate	33.3	Very high	Qal
76	449,701	4,443,792	3.40	58	Moderate	17.0	Very high	Qal
77	450,435	4,444,621	3.60	77	High	32.5	Very high	Qal
78	450,194	4,443,809	3.20	95	Very high	42.5	Very high	Qal
79	450,430	4,444,070	4.40	96	Very high	38.3	Very high	Qal
80	450,170	4,445,234	2.15	39	Moderate	9.4	High	Qal
81	449,932	4,443,951	3.20	50	Moderate	19.1	Very high	Qal
82	449,889	4,443,710	3.25	70	High	33.7	Very high	Qal
83	449,688	4,443,519	1.80	68	High	36.1	Very high	Qal
84	450,355	4,444,857	1.80	83	High	39.3	Very high	Qal
85	450,095	4,443,946	3.50	95	Very high	36.8	Very high	Qal
86	450,353	4,444,408	4.15	65	High	29.6	Very high	Qal
87	450,580	4,444,884	2.30	17	Low	6.8	High	Qal
88	449,957	4,443,410	1.80	73	High	38.6	Very high	Qal
89	449,757	4,443,340	1.80	66	High	31.2	Very high	Qal
90	449,939	4,443,238	1.85	74	High	38.9	Very high	Qal
91	449,295	4,444,655	1.80	72	High	42.6	Very high	Qal
92	450,027	4,444,917	2.40	62	Moderate	28.5	Very high	Qal
93	450,200	4,444,640	3.60	66	High	30.9	Very high	Qal
94	449,373	4,443,741	1.30	75	High	40.5	Very high	Qal
95	449,633	4,443,109	1.80	73	High	35.8	Very high	Qal
96	450,225	4,444,516	3.45	72	High	42	Very high	Qal
97	449,876	4,442,887	1.80	73	High	37.8	Very high	Qal
98	449,753	4,442,961	1.80	73	High	40.2	Very high	Qal
99	449,482	4,442,975	1.80	77	High	47	Very high	Qal
100	449,183	4,444,800	1.15	73	High	41	Very high	Qal

Table 7 (continued)

Borehole no.	Coordinates		Depth of GWT (m)	L_S	Description	LPI	Description	Fm
	N	E						
101	449,607	4,442,703	2.00	74	High	40.4	Very high	Qal
102	449,768	4,442,569	2.50	75	High	40.9	Very high	Qal
103	449,657	4,442,205	0.75	77	High	50.6	Very high	Qal
104	449,744	4,441,830	0.60	77	High	50.6	Very high	Qal
105	449,910	4,441,405	1.00	78	High	60.9	Very high	Qal
106	449,744	4,441,147	0.65	77	High	50.6	Very high	Qal
107	449,535	4,443,815	1.50	61	Moderate	37	Very high	Qal
108	449,567	4,444,856	1.75	66	High	20.2	Very high	Qal
109	449,370	4,443,617	2.00	70	High	35	Very high	Qal
110	449,637	4,444,262	2.60	65	High	39	Very high	Qal
111	449,785	4,444,169	2.75	76	High	44	Very high	Qal
112	449,420	4,444,068	1.20	76	High	45.2	Very high	Qal
113	450,407	4,444,945	2.05	67	High	31	Very high	Qal
114	449,017	4,444,121	0.90	77	High	48.7	Very high	Qal
115	450,568	4,445,277	3.70	0	Non-liquefiable	0	Non-liquefiable	Tmal
116	450,461	4,445,539	6.85	0	Non-liquefiable	0	Non-liquefiable	Tmal
117	450,619	4,445,451	8.20	0	Non-liquefiable	0	Non-liquefiable	Tmal
118	449,871	4,444,257	3.00	74	High	38	Very high	Qal
119	450,490	4,445,041	2.45	42	Moderate	11.4	High	Qal
120	450,031	4,444,392	3.60	73	High	37	Very high	Qal
121	449,996	4,444,209	3.70	67	High	29	Very high	Qal
122	449,199	4,444,277	2.30	66	High	33.5	Very high	Qal
123	449,803	4,444,394	3.00	75	High	40.1	Very high	Qal
124	449,789	4,444,470	2.90	74	High	38.1	Very high	Qal
125	451,438	4,445,992	9.90	46	Moderate	1.7	Low	Qal
126	451,194	4,446,344	9.80	37	Moderate	8.7	High	Qal
127	449,988	4,446,040	6.95	0	Non-liquefiable	0	Non-liquefiable	Tmal
128	450,909	4,446,669	7.45	38	Moderate	10.4	High	Qal
129	450,083	4,446,184	0.75	0	Non-liquefiable	0	Non-liquefiable	Tmal
130	450,469	4,446,065	4.30	0	Non-liquefiable	0	Non-liquefiable	Tmal
131	450,679	4,446,368	4.30	0	Non-liquefiable	0	Non-liquefiable	Tmal
132	449,699	4,446,302	No Water	0	Non-liquefiable	0	Non-liquefiable	Tmal
133	450,799	4,446,063	No Water	0	Non-liquefiable	0	Non-liquefiable	Tmal
134	449,916	4,446,566	2.40	0	Non-liquefiable	0	Non-liquefiable	Tmal
135	450,142	4,446,738	No water	0	Non-liquefiable	0	Non-liquefiable	Tmal
136	450,451	4,446,770	No water	0	Non-liquefiable	0	Non-liquefiable	Tmal
137	450,429	4,446,437	0.70	0	Non-liquefiable	0	Non-liquefiable	Tmal
138	451,157	4,445,715	5.40	0	Non-liquefiable	0	Non-liquefiable	Tmal
139	450,098	4,445,736	No water	0	Non-liquefiable	0	Non-liquefiable	Tmal
140	449,890	4,445,647	4.45	0	Non-liquefiable	0	Non-liquefiable	Tmal
141	450,236	4,444,045	4.4	74	High	32.2	Very high	Qal
142	450,860	4,447,173	1.90	0	Non-liquefiable	0	Non-liquefiable	Qal
143	449,878	4,445,344	2.00	95	Very high	50.6	Very high	Qal
144	452,074	4,446,440	No water	0	Non-liquefiable	0	Non-liquefiable	Tmal
145	449,580	4,443,463	2.00	72	High	51.3	Very high	Qal
146	448,982	4,443,831	1.15	77	High	48.7	Very high	Qal
147	449,968	4,444,573	2.45	80	High	57.3	Very high	Qal
148	450,687	4,445,841	2.35	0	Non-liquefiable	0	Non-liquefiable	Tmal
149	449,746	4,444,576	1.45	80	High	51.3	Very high	Qal
150	449,208	4,444,740	1.15	76	High	44.2	Very high	Qal
151	448,946	4,444,715	1.00	66	High	37.1	Very high	Qal

Table 8 Liquefaction severity index (L_S) and liquefaction potential index (LPI) values for a_{max} = 222 gal (Fm: formation, Qal: alluvium, Tmal: alcitepe Fm, and Tmg: gazhanedere Fm)

Borehole no.	Coordinates		Depth of GWT (m)	L_S	Description	LPI	Description	Fm
	N	E						
1	453,172	4,444,526	3.50	22	Low	8.4	High	Qal
2	452,983	4,444,163	6.10	50	Moderate	19.3	Very high	Qal
3	453,215	4,444,145	4.00	50	Moderate	19.3	Very high	Qal
4	453,315	4,444,364	4.70	6	Very Low	1.4	Low	Qal
5	452,794	4,444,079	6.00	29	Low	6.8	High	Qal
6	452,793	4,444,251	6.00	24	Low	6.9	High	Qal
7	452,794	4,444,725	3.50	37	Moderate	6.9	High	Qal
8	452,660	4,444,599	2.10	36	Moderate	7.1	High	Qal
9	452,503	4,444,288	5.50	48	Moderate	11.6	High	Qal
10	452,339	4,444,055	2.60	58	Moderate	18.7	Very high	Qal
11	452,226	4,444,226	3.65	48	Moderate	13.8	High	Qal
12	452,292	4,444,519	4.00	66	High	27.3	Very high	Qal
13	452,108	4,444,698	1.80	51	Moderate	13.2	High	Qal
14	451,973	4,444,686	2.30	45	Moderate	10.2	High	Qal
15	451,949	4,444,491	3.80	48	Moderate	9.9	High	Qal
16	452,062	4,444,267	4.40	48	Moderate	16.1	Very high	Qal
17	451,777	4,444,522	5.30	48	Moderate	12.8	High	Qal
18	451,620	4,444,265	4.40	53	Moderate	15.2	Very high	Qal
19	451,485	4,444,469	2.50	57	Moderate	30.4	Very high	Qal
20	451,241	4,444,704	5.20	54	Moderate	17.1	Very high	Qal
21	451,068	4,444,477	4.55	53	Moderate	13.5	High	Qal
22	450,947	4,444,381	4.25	56	Moderate	24.3	Very high	Qal
23	451,256	4,444,402	5.35	45	Moderate	6.4	High	Qal
24	451,244	4,444,170	5.10	63	Moderate	26.5	Very high	Qal
25	451,043	4,444,160	5.10	59	Moderate	25.4	Very high	Qal
26	450,800	4,444,193	5.10	59	Moderate	25.4	Very high	Qal
27	450,642	4,444,299	5.30	58	Moderate	24.5	Very high	Qal
28	450,665	4,444,453	4.50	52	Moderate	16.6	Very high	Qal
29	450,823	4,444,468	3.60	56	Moderate	17.4	Very high	Qal
30	450,971	4,444,613	2.90	58	Moderate	18.1	Very high	Qal
31	450,701	4,444,667	3.55	18	Low	2.6	Moderate	Qal
32	450,726	4,444,758	2.60	17	Low	3.2	Moderate	Qal
33	450,736	4,444,592	3.70	53	Moderate	21.2	Very high	Qal
34	450,601	4,444,536	3.50	27	Low	10.2	High	Qal
35	450,374	4,441,102	1.10	0	Non-liquefiable	0	Non-liquefiable	Tmg
36	450,210	4,441,280	5.25	22	Very Low	0	Non-liquefiable	Qal
37	450,024	4,441,320	3.10	47	Moderate	17.1	Very high	Qal
38	450,588	4,441,537	4.00	0	Non-liquefiable	0	Non-liquefiable	Tmg
39	450,319	4,441,673	7.00	39	Moderate	6.1	High	Qal
40	449,836	4,442,074	2.00	52	Moderate	15.8	Very high	Qal
41	450,096	4,442,251	3.00	46	Moderate	14	High	Qal
42	450,053	4,442,420	2.90	63	Moderate	24.8	Very high	Qal
43	450,198	4,442,580	0.65	60	Moderate	21.7	Very high	Qal
44	450,036	4,442,644	2.55	70	High	34	Very high	Qal
45	450,156	4,442,700	1.40	69	High	45.8	Very high	Qal
46	450,015	4,442,727	2.10	37	Moderate	13.9	High	Qal
47	450,255	4,442,830	1.90	57	Moderate	24	Very high	Qal
48	450,105	4,442,945	2.00	62	Moderate	23.8	Very high	Qal
49	450,022	4,443,004	2.00	42	Moderate	8.4	High	Qal

Table 8 (continued)

Borehole no.	Coordinates		Depth of GWT (m)	L_S	Description	LPI	Description	Fm
	N	E						
50	450,249	4,442,981	2.20	69	High	31.7	Very high	Qal
51	450,393	4,443,028	1.90	41	Moderate	10.9	High	Qal
52	450,131	4,443,155	2.35	49	Moderate	17	Very high	Qal
53	450,160	4,443,279	2.40	67	High	23.5	Very high	Qal
54	450,345	4,443,331	2.45	58	Moderate	19.5	Very high	Qal
55	450,618	4,443,173	2.75	78	High	34.5	Very high	Qal
56	450,155	4,443,491	2.20	78	High	34.6	Very high	Qal
57	450,670	4,443,392	3.30	80	High	39.2	Very high	Qal
58	450,446	4,443,543	4.00	79	High	32.5	Very high	Qal
59	450,697	4,443,568	3.15	60	Moderate	25.7	Very high	Qal
60	450,316	4,443,623	3.00	66	High	24.7	Very high	Qal
61	450,607	4,443,536	3.40	79	High	35.5	Very high	Qal
62	450,795	4,443,722	4.50	54	Moderate	17.1	Very high	Qal
63	450,917	4,443,830	2.55	26	Low	10.3	High	Qal
64	450,668	4,443,815	4.45	63	Moderate	18.5	Very high	Qal
65	450,484	4,443,850	3.90	67	High	22.6	Very high	Qal
66	450,541	4,443,941	3.80	47	Moderate	9	High	Qal
67	450,812	4,444,007	4.60	57	Moderate	16	Very high	Qal
68	450,963	4,443,908	3.55	21	Low	0	Non-liquefiable	Qal
69	449,297	4,443,959	1.55	22	Low	4.7	Moderate	Qal
70	449,774	4,444,380	3.50	47	Moderate	10.6	High	Qal
71	449,072	4,443,939	1.40	29	Low	2.7	Moderate	Qal
72	449,419	4,443,315	2.40	64	Moderate	26.7	Very high	Qal
73	449,012	4,443,662	1.10	35	Moderate	4.3	Moderate	Qal
74	448,945	4,443,847	0.80	29	Low	2.8	Moderate	Qal
75	449,236	4,443,892	1.95	42	Moderate	11	High	Qal
76	449,701	4,443,792	3.40	24	Low	4.1	Moderate	Qal
77	450,435	4,444,621	3.60	57	Moderate	18.6	High	Qal
78	450,194	4,443,809	3.20	69	High	19.7	Very high	Qal
79	450,430	4,444,070	4.40	74	High	23.7	Very high	Qal
80	450,170	4,445,234	2.15	22	Low	5.7	High	Qal
81	449,932	4,443,951	3.20	21	Low	3.4	Moderate	Qal
82	449,889	4,443,710	3.25	40	Moderate	7.9	High	Qal
83	449,688	4,443,519	1.80	45	Moderate	15.9	Very high	Qal
84	450,355	4,444,857	1.80	58	Moderate	21.3	Very high	Qal
85	450,095	4,443,946	3.50	67	High	18	Very high	Qal
86	450,353	4,444,408	4.15	47	Moderate	13.4	High	Qal
87	450,580	4,444,884	2.30	11	Very Low	2.1	Low	Qal
88	449,957	4,443,410	1.80	47	Moderate	12.5	High	Qal
89	449,757	4,443,340	1.80	43	Moderate	15.9	Very high	Qal
90	449,939	4,443,238	1.85	48	Moderate	11.6	High	Qal
91	449,295	4,444,655	1.80	64	Moderate	28.4	Very high	Qal
92	450,027	4,444,917	2.40	44	Moderate	13	High	Qal
93	450,200	4,444,640	3.60	49	Moderate	16.9	Very high	Qal
94	449,373	4,443,741	1.30	51	Moderate	14	High	Qal
95	449,633	4,443,109	1.80	67	High	27.7	Very high	Qal
96	450,225	4,444,516	3.45	61	Moderate	28.5	Very high	Qal
97	449,876	4,442,887	1.80	46	Moderate	12	High	Qal
98	449,753	4,442,961	1.80	51	Moderate	17.7	Very high	Qal
99	449,482	4,442,975	1.80	63	Moderate	24.4	Very high	Qal
100	449,183	4,444,800	1.15	61	Moderate	25	Very high	Qal

Table 8 (continued)

Borehole no.	Coordinates		Depth of GWT (m)	L_S	Description	LPI	Description	Fm
	N	E						
101	449,607	4,442,703	2.00	49	Moderate	14.9	High	Qal
102	449,768	4,442,569	2.50	52	Moderate	14	High	Qal
103	449,657	4,442,205	0.75	66	High	30.6	Very high	Qal
104	449,744	4,441,830	0.60	66	High	30.6	Very high	Qal
105	449,910	4,441,405	1.00	75	High	53.4	Very high	Qal
106	449,744	4,441,147	0.65	64	Moderate	30.5	Very high	Qal
107	449,535	4,443,815	1.50	49	Moderate	20.5	Very high	Qal
108	449,567	4,444,856	1.75	39	Moderate	7.2	High	Qal
109	449,370	4,443,617	2.00	42	Moderate	11.5	High	Qal
110	449,637	4,444,262	2.60	59	Moderate	27.1	Very high	Qal
111	449,785	4,444,169	2.75	67	High	28.7	Very high	Qal
112	449,420	4,444,068	1.20	68	High	30.4	Very high	Qal
113	450,407	4,444,945	2.05	48	Moderate	13.8	High	Qal
114	449,017	4,444,121	0.90	72	High	35.6	Very high	Qal
115	450,568	4,445,277	3.70	0	Non-liquefiable	0	Non-liquefiable	Tmal
116	450,461	4,445,539	6.85	0	Non-liquefiable	0	Non-liquefiable	Tmal
117	450,619	4,445,451	8.20	0	Non-liquefiable	0	Non-liquefiable	Tmal
118	449,871	4,444,257	3.00	59	Moderate	20.2	Very high	Qal
119	450,490	4,445,041	2.45	19	Low	1.5	Low	Qal
120	450,031	4,444,392	3.60	57	Moderate	18.6	Very high	Qal
121	449,996	4,444,209	3.70	44	Moderate	9.5	High	Qal
122	449,199	4,444,277	2.30	52	Moderate	21.4	Very high	Qal
123	449,803	4,444,394	3.00	62	Moderate	23.3	Very high	Qal
124	449,789	4,444,470	2.90	59	Moderate	20.3	Very high	Qal
125	451,438	4,445,992	9.90	18	Low	0.3	Low	Qal
126	451,194	4,446,344	9.80	16	Low	1.3	Low	Qal
127	449,988	4,446,040	6.95	0	Non-liquefiable	0	Non-liquefiable	Tmal
128	450,909	4,446,669	7.45	27	Low	2.7	Moderate	Qal
129	450,083	4,446,184	0.75	0	Non-liquefiable	0	Non-liquefiable	Tmal
130	450,469	4,446,065	4.30	0	Non-liquefiable	0	Non-liquefiable	Tmal
131	450,679	4,446,368	4.30	0	Non-liquefiable	0	Non-liquefiable	Tmal
132	449,699	4,446,302	No water	0	Non-liquefiable	0	Non-liquefiable	Tmal
133	450,799	4,446,063	No water	0	Non-liquefiable	0	Non-liquefiable	Tmal
134	449,916	4,446,566	2.40	0	Non-liquefiable	0	Non-liquefiable	Tmal
135	450,142	4,446,738	No water	0	Non-liquefiable	0	Non-liquefiable	Tmal
136	450,451	4,446,770	No water	0	Non-liquefiable	0	Non-liquefiable	Tmal
137	450,429	4,446,437	0.70	0	Non-liquefiable	0	Non-liquefiable	Tmal
138	451,157	4,445,715	5.40	0	Non-liquefiable	0	Non-liquefiable	Tmal
139	450,098	4,445,736	No water	0	Non-liquefiable	0	Non-liquefiable	Tmal
140	449,890	4,445,647	4.45	0	Non-liquefiable	0	Non-liquefiable	Tmal
141	450,236	4,444,045	4.4	51	Moderate	15.8	Very high	Qal
142	450,860	4,447,173	1.90	0	Non-liquefiable	0	Non-liquefiable	Qal
143	449,878	4,445,344	2.00	82	High	32.2	Very high	Qal
144	452,074	4,446,440	No water	0	Non-liquefiable	0	Non-liquefiable	Tmal
145	449,580	4,443,463	2.00	68	High	36.1	Very high	Qal
146	448,982	4,443,831	1.15	72	High	35.5	Very high	Qal
147	449,968	4,444,573	2.45	83	High	41.9	Very high	Qal
148	450,687	4,445,841	2.35	0	Non-liquefiable	0	Non-liquefiable	Tmal
149	449,746	4,444,576	1.45	73	High	36.3	Very high	Qal
150	449,208	4,444,740	1.15	66	High	29	Very high	Qal
151	448,946	4,444,715	1.00	55	Moderate	23	Very high	Qal

Table 9 Liquefaction severity index (L_S) and liquefaction potential index (LPI) values for a_{max} = 141 gal (Fm: formation, Qal: alluvium, Tmal: alcitepe Fm, and Tmg: gazhanedere Fm)

Borehole no.	Coordinates		Depth of GWT (m)	L_S	Description	LPI	Description	Fm
	N	E						
1	453,172	4,444,526	3.50	15	Low	2.6	Moderate	Qal
2	452,983	4,444,163	6.10	25	Low	4.3	Moderate	Qal
3	453,215	4,444,145	4.00	35.5	Moderate	7.5	High	Qal
4	453,315	4,444,364	4.70	3	Very low	0	Non-liquefiable	Qal
5	452,794	4,444,079	6.00	16	Low	2.7	Moderate	Qal
6	452,793	4,444,251	6.00	14.8	Very low	2.8	Moderate	Qal
7	452,794	4,444,725	3.50	18	Low	2	Low	Qal
8	452,660	4,444,599	2.10	26	Low	3.2	Moderate	Qal
9	452,503	4,444,288	5.50	42	Moderate	8.8	High	Qal
10	452,339	4,444,055	2.60	37	Moderate	4.6	Moderate	Qal
11	452,226	4,444,226	3.65	30	Moderate	6	High	Qal
12	452,292	4,444,519	4.00	36	Moderate	6.1	High	Qal
13	452,108	4,444,698	1.80	30	Low	6.0	High	Qal
14	451,973	4,444,686	2.30	31	Low	4.1	Moderate	Qal
15	451,949	4,444,491	3.80	34	Low	4.6	Moderate	Qal
16	452,062	4,444,267	4.40	47	Moderate	6.8	High	Qal
17	451,777	4,444,522	5.30	14.6	Very low	0.2	Low	Qal
18	451,620	4,444,265	4.40	32	Low	2.7	Moderate	Qal
19	451,485	4,444,469	2.50	44	Moderate	16.8	Very high	Qal
20	451,241	4,444,704	5.20	34	Low	6.6	High	Qal
21	451,068	4,444,477	4.55	31	Low	4.3	Moderate	Qal
22	450,947	4,444,381	4.25	47	Moderate	12.5	High	Qal
23	451,256	4,444,402	5.35	22	Low	0.9	Low	Qal
24	451,244	4,444,170	5.10	40	Moderate	12.6	High	Qal
25	451,043	4,444,160	5.10	48	Moderate	17.4	Very high	Qal
26	450,800	4,444,193	5.10	34	Low	7.4	High	Qal
27	450,642	4,444,299	5.30	45	Moderate	14.8	High	Qal
28	450,665	4,444,453	4.50	42	Moderate	9.6	High	Qal
29	450,823	4,444,468	3.60	35.5	Moderate	5.7	High	Qal
30	450,971	4,444,613	2.90	35.5	Moderate	4.4	Moderate	Qal
31	450,701	4,444,667	3.55	8	Very low	0.3	Low	Qal
32	450,726	4,444,758	2.60	8	Very low	0.3	Low	Qal
33	450,736	4,444,592	3.70	51	Moderate	14.3	High	Qal
34	450,601	4,444,536	3.50	19	Low	3.5	Moderate	Qal
35	450,374	4,441,102	1.10	0	Non-liquefiable	0	Non-liquefiable	Tmg
36	450,210	4,441,280	5.25	5	Very low	0	Non-liquefiable	Qal
37	450,024	4,441,320	3.10	23	Low	2.7	Moderate	Qal
38	450,588	4,441,537	4.00	0	Non-liquefiable	0	Non-liquefiable	Tmg
39	450,319	4,441,673	7.00	7	Very low	0.1	Low	Qal
40	449,836	4,442,074	2.00	20	Low	0.8	Low	Qal
41	450,096	4,442,251	3.00	18	Low	1.3	Low	Qal
42	450,053	4,442,420	2.90	33	Low	5.4	High	Qal
43	450,198	4,442,580	0.65	28	Low	2	Moderate	Qal
44	450,036	4,442,644	2.55	49	Moderat	18.2	Very high	Qal
45	450,156	4,442,700	1.40	64	Moderate	27.3	Very high	Qal
46	450,015	4,442,727	2.10	19.5	Low	3.7	Moderate	Qal
47	450,255	4,442,830	1.90	33	Low	7.6	High	Qal
48	450,105	4,442,945	2.00	31	Low	4.9	Moderate	Qal
49	450,022	4,443,004	2.00	12	Very low	0.2	Low	Qal

Table 9 (continued)

Borehole no.	Coordinates		Depth of GWT (m)	L_S	Description	LPI	Description	Fm
	N	E						
50	450,249	4,442,981	2.20	42.5	Moderate	10.3	High	Qal
51	450,393	4,443,028	1.90	17	Low	3.0	Moderate	Qal
52	450,131	4,443,155	2.35	26	Low	5.7	High	Qal
53	450,160	4,443,279	2.40	31	Low	3.5	Moderate	Qal
54	450,345	4,443,331	2.45	30	Low	1.8	Low	Qal
55	450,618	4,443,173	2.75	51	Moderate	14.5	High	Qal
56	450,155	4,443,491	2.20	49	Moderate	14.7	High	Qal
57	450,670	4,443,392	3.30	56	Moderate	16.7	Very high	Qal
58	450,446	4,443,543	4.00	44	Moderate	7.2	High	Qal
59	450,697	4,443,568	3.15	34	Low	6.7	High	Qal
60	450,316	4,443,623	3.00	34	Low	6	High	Qal
61	450,607	4,443,536	3.40	49	Moderate	10.6	High	Qal
62	450,795	4,443,722	4.50	24	Low	3.9	Moderate	Qal
63	450,917	4,443,830	2.55	14	Low	2.6	Moderate	Qal
64	450,668	4,443,815	4.45	25	Low	2	Low	Qal
65	450,484	4,443,850	3.90	28	Low	2.5	Moderate	Qal
66	450,541	4,443,941	3.80	14	Very low	0.3	Low	Qal
67	450,812	4,444,007	4.60	21	Low	1.6	Low	Qal
68	450,963	4,443,908	3.55	3	Very low	0	Non-liquefiable	Qal
69	449,297	4,443,959	1.55	11	Very low	1.1	Low	Qal
70	449,774	4,444,380	3.50	11	Very low	0.8	Low	Qal
71	449,072	4,443,939	1.40	13	Very low	0.3	Low	Qal
72	449,419	4,443,315	2.40	48	Moderate	11.3	High	Qal
73	449,012	4,443,662	1.10	17	Low	0.4	Low	Qal
74	448,945	4,443,847	0.80	12	Very low	0.2	Low	Qal
75	449,236	4,443,892	1.95	23	Low	1.1	Low	Qal
76	449,701	4,443,792	3.40	11	Very low	0.5	Low	Qal
77	450,435	4,444,621	3.60	24	Low	2.2	Moderate	Qal
78	450,194	4,443,809	3.20	33	Low	2.9	Moderate	Qal
79	450,430	4,444,070	4.40	40	Moderate	5.3	High	Qal
80	450,170	4,445,234	2.15	9	Very low	2.3	Moderate	Qal
81	449,932	4,443,951	3.20	10	Very low	0.9	Low	Qal
82	449,889	4,443,710	3.25	20	Low	0.8	Low	Qal
83	449,688	4,443,519	1.80	31	Low	8.4	High	Qal
84	450,355	4,444,857	1.80	30	Low	10.1	High	Qal
85	450,095	4,443,946	3.50	39	Moderat	3.8	Moderate	Qal
86	450,353	4,444,408	4.15	18	Low	0.8	Low	Qal
87	450,580	4,444,884	2.30	3	Very low	0	Non-liquefiable	Qal
88	449,957	4,443,410	1.80	28	Low	4.4	Moderate	Qal
89	449,757	4,443,340	1.80	29	Low	6.1	High	Qal
90	449,939	4,443,238	1.85	26	Low	3.8	Moderate	Qal
91	449,295	4,444,655	1.80	38	Moderate	6.9	High	Qal
92	450,027	4,444,917	2.40	17	Low	0.5	Low	Qal
93	450,200	4,444,640	3.60	22	Low	1.4	Low	Qal
94	449,373	4,443,741	1.30	30	Low	4	Moderate	Qal
95	449,633	4,443,109	1.80	21	Low	1.4	Low	Qal
96	450,225	4,444,516	3.45	40	Moderate	12	High	Qal
97	449,876	4,442,887	1.80	27	Low	3.8	Moderate	Qal
98	449,753	4,442,961	1.80	34	Low	5.9	High	Qal
99	449,482	4,442,975	1.80	44	Moderate	10.2	High	Qal
100	449,183	4,444,800	1.15	36	Moderate	7.9	High	Qal

Table 9 (continued)

Borehole no.	Coordinates		Depth of GWT (m)	L_S	Description	LPI	Description	Fm
	N	E						
101	449,607	4,442,703	2.00	31.5	Low	7.7	High	Qal
102	449,768	4,442,569	2.50	30.5	Low	3.6	Moderate	Qal
103	449,657	4,442,205	0.75	51	Moderate	16.9	Very high	Qal
104	449,744	4,441,830	0.60	49.5	Moderate	18.4	Very high	Qal
105	449,910	4,441,405	1.00	69	High	40.9	Very high	Qal
106	449,744	4,441,147	0.65	49.5	Moderate	18.5	Very high	Qal
107	449,535	4,443,815	1.50	38	Moderate	10.4	High	Qal
108	449,567	4,444,856	1.75	11	Very low	0.7	Low	Qal
109	449,370	4,443,617	2.00	25	Low	3.1	Moderate	Qal
110	449,637	4,444,262	2.60	36	Moderate	6.8	High	Qal
111	449,785	4,444,169	2.75	38	Moderate	6.6	High	Qal
112	449,420	4,444,068	1.20	40	Moderate	7.2	High	Qal
113	450,407	4,444,945	2.05	17	Low	0.8	Low	Qal
114	449,017	4,444,121	0.90	49	Moderate	11.8	High	Qal
115	450,568	4,445,277	3.70	0	Non-liquefiable	0	Non-liquefiable	Tmal
116	450,461	4,445,539	6.85	0	Non-liquefiable	0	Non-liquefiable	Tmal
117	450,619	4,445,451	8.20	0	Non-liquefiable	0	Non-liquefiable	Tmal
118	449,871	4,444,257	3.00	24	Low	1.1	Low	Qal
119	450,490	4,445,041	2.45	4	Very low	0	Non-liquefiable	Qal
120	450,031	4,444,392	3.60	22	Low	1	Low	Qal
121	449,996	4,444,209	3.70	14	Very low	0.8	Low	Qal
122	449,199	4,444,277	2.30	29	Low	6.4	High	Qal
123	449,803	4,444,394	3.00	28	Low	3.6	Moderate	Qal
124	449,789	4,444,470	2.90	25	Low	1.6	Low	Qal
125	451,438	4,445,992	9.90	3	Very low	0	Non-liquefiable	Qal
126	451,194	4,446,344	9.80	3	Very low	1.4	Low	Qal
127	449,988	4,446,040	6.95	0	Non-liquefiable	0	Non-liquefiable	Tmal
128	450,909	4,446,669	7.45	3	Very low	0	Non-liquefiable	Qal
129	450,083	4,446,184	0.75	0	Non-liquefiable	0	Non-liquefiable	Tmal
130	450,469	4,446,065	4.30	0	Non-liquefiable	0	Non-liquefiable	Tmal
131	450,679	4,446,368	4.30	0	Non-liquefiable	0	Non-liquefiable	Tmal
132	449,699	4,446,302	No water	0	Non-liquefiable	0	Non-liquefiable	Tmal
133	450,799	4,446,063	No water	0	Non-liquefiable	0	Non-liquefiable	Tmal
134	449,916	4,446,566	2.40	0	Non-liquefiable	0	Non-liquefiable	Tmal
135	450,142	4,446,738	No water	0	Non-liquefiable	0	Non-liquefiable	Tmal
136	450,451	4,446,770	No water	0	Non-liquefiable	0	Non-liquefiable	Tmal
137	450,429	4,446,437	0.70	0	Non-liquefiable	0	Non-liquefiable	Tmal
138	451,157	4,445,715	5.40	0	Non-liquefiable	0	Non-liquefiable	Tmal
139	450,098	4,445,736	No water	0	Non-liquefiable	0	Non-liquefiable	Tmal
140	449,890	4,445,647	4.45	0	Non-liquefiable	0	Non-liquefiable	Tmal
141	450,236	4,444,045	4.4	28	Low	5.9	High	Qal
142	450,860	4,447,173	1.90	0	Non-liquefiable	0	Non-liquefiable	Qal
143	449,878	4,445,344	2.00	42	Moderate	5.2	High	Qal
144	452,074	4,446,440	No water	0	Non-liquefiable	0	Non-liquefiable	Tmal
145	449,580	4,443,463	2.00	60	Moderate	24.6	Very high	Qal
146	448,982	4,443,831	1.15	49	Moderate	11.9	High	Qal
147	449,968	4,444,573	2.45	60	Moderate	13.6	High	Qal
148	450,687	4,445,841	2.35	0	Non-liquefiable	0	Non-liquefiable	Tmal
149	449,746	4,444,576	1.45	52	Moderate	21.2	Very high	Qal
150	449,208	4,444,740	1.15	38	Moderate	8.7	High	Qal
151	448,946	4,444,715	1.00	28	Low	7.3	High	Qal

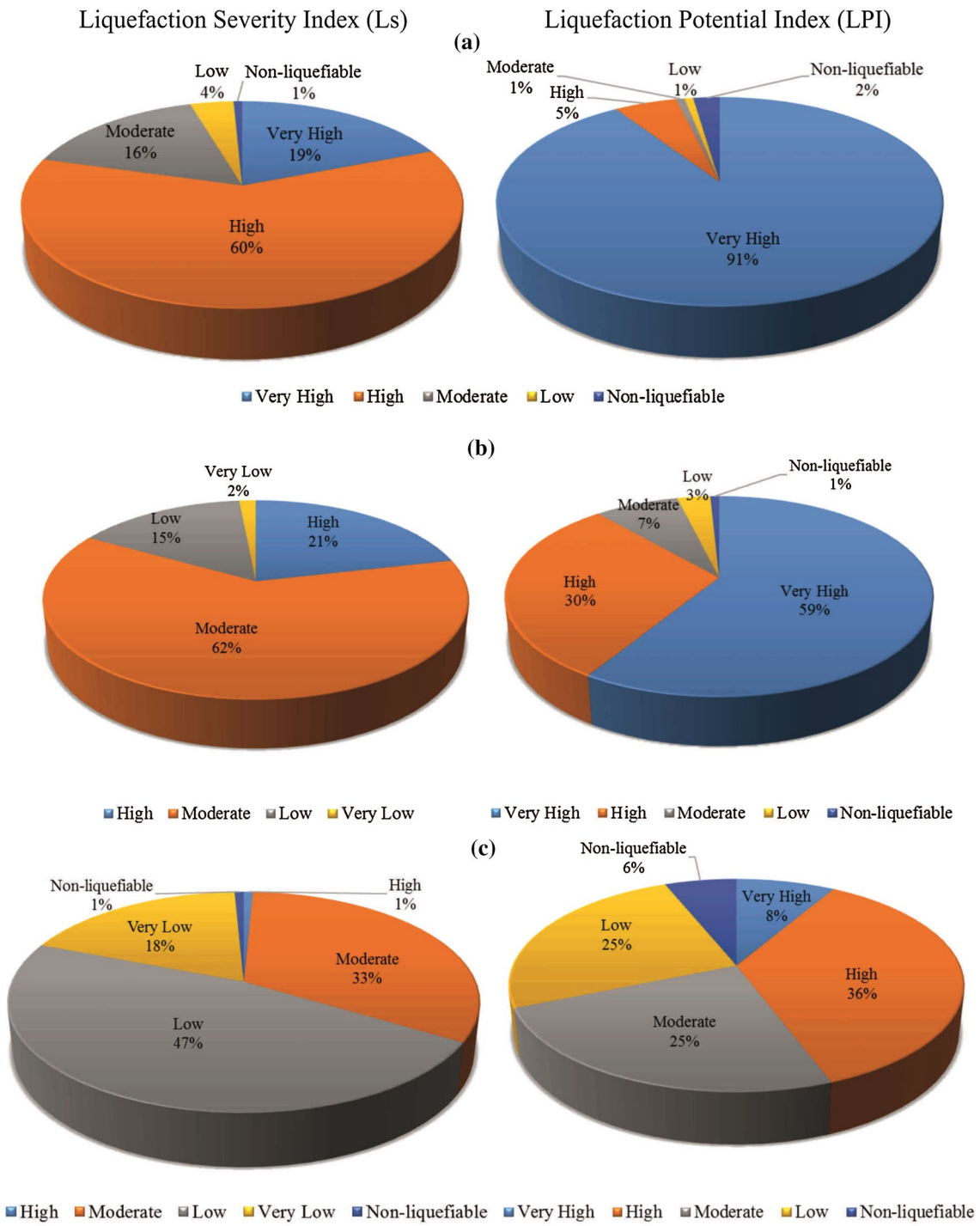

Fig. 11 Pie charts showing the areas of the liquefaction severity index and liquefaction potential index. **a** a_{max} = 319 gal, **b** a_{max} = 222 gal, and **c** a_{max} = 141 gal

value measured at the Canakkale station during the 2014 Aegean Sea earthquake was used to analyse these two methods. In addition, the possible environmental impacts of liquefaction were discussed. The main results obtained are the following:

1. The Quaternary alluvial deposits are generally susceptible to liquefaction and cover most of the Canakkale settlement area. It was also determined that the groundwater level is rather shallow. In addition, Canakkale city is located in a seismically active region in Turkey. All

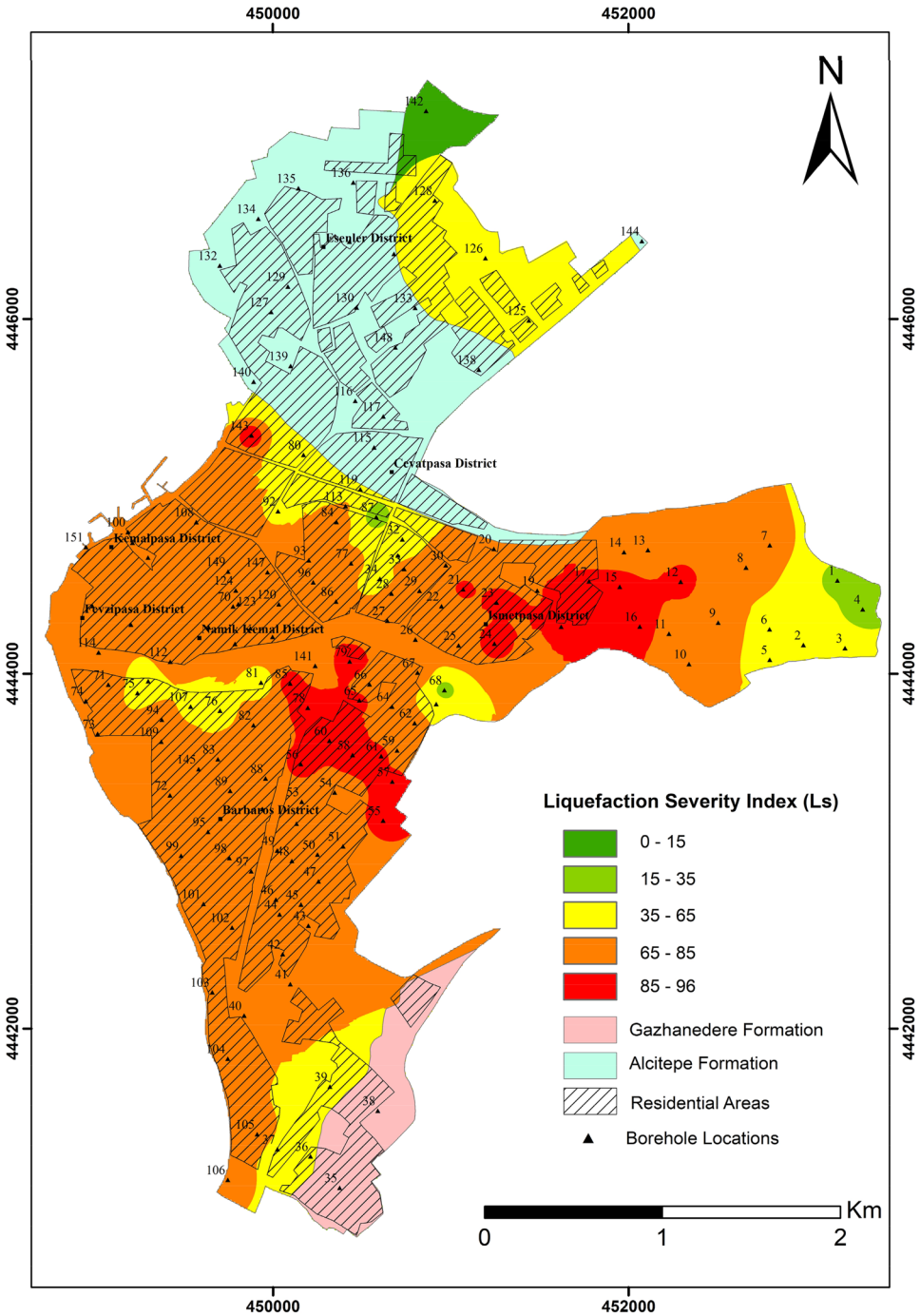

Fig. 12 Liquefaction severity map (a_{max} = 319 gal)

these conditions are compatible with the occurrence of the liquefaction phenomenon.

2. The liquefaction severity and liquefaction potential index maps for the Canakkale settlement area were prepared. According to the liquefaction severity index for a_{max} = 319 gal, the category of very high and high susceptibility for liquefaction was observed in the eastern and south parts of Canakkale city. The moderate category of the liquefaction severity index was mainly observed at the centre, the southern, and the eastern parts of Canakkale city for the a_{max} = 222 gal.

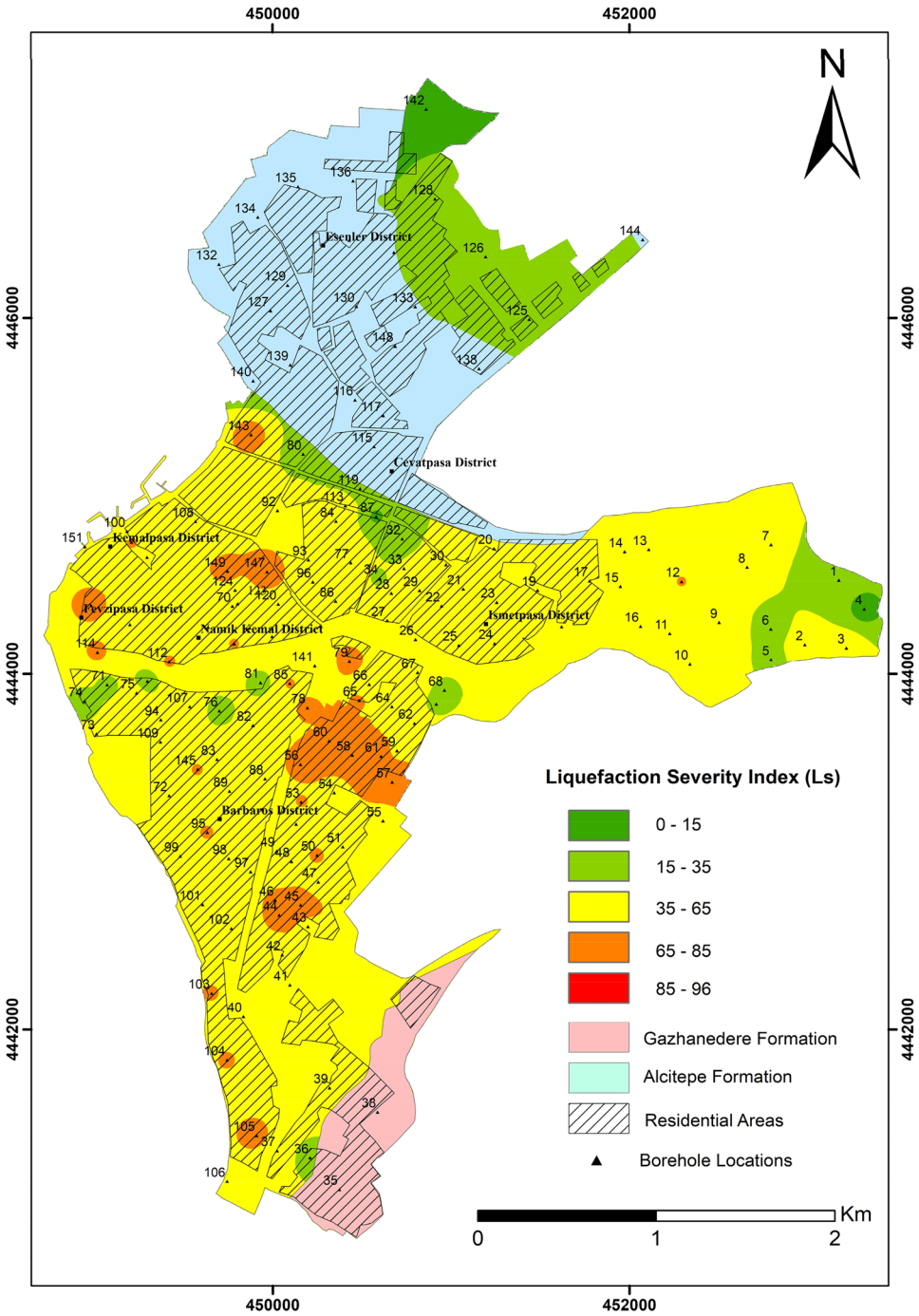

Fig. 13 Liquefaction severity map (a_{max} = 222 gal)

3. According to the liquefaction potential index, almost all of the alluvial deposits are in the very high liquefaction category for a_{max} = 319 gal. The category of very high liquefaction potential was mainly observed at the centre and the southern parts of Canakkale city for the a_{max} = 222 gal.
4. Almost all of the Quaternary alluvial deposits are in the category of moderate and low for a_{max} = 141 gal according to the liquefaction severity index. However, according to the liquefaction potential index, the Quaternary alluvial deposits are in the category of high and moderate for the same peak ground acceleration value.

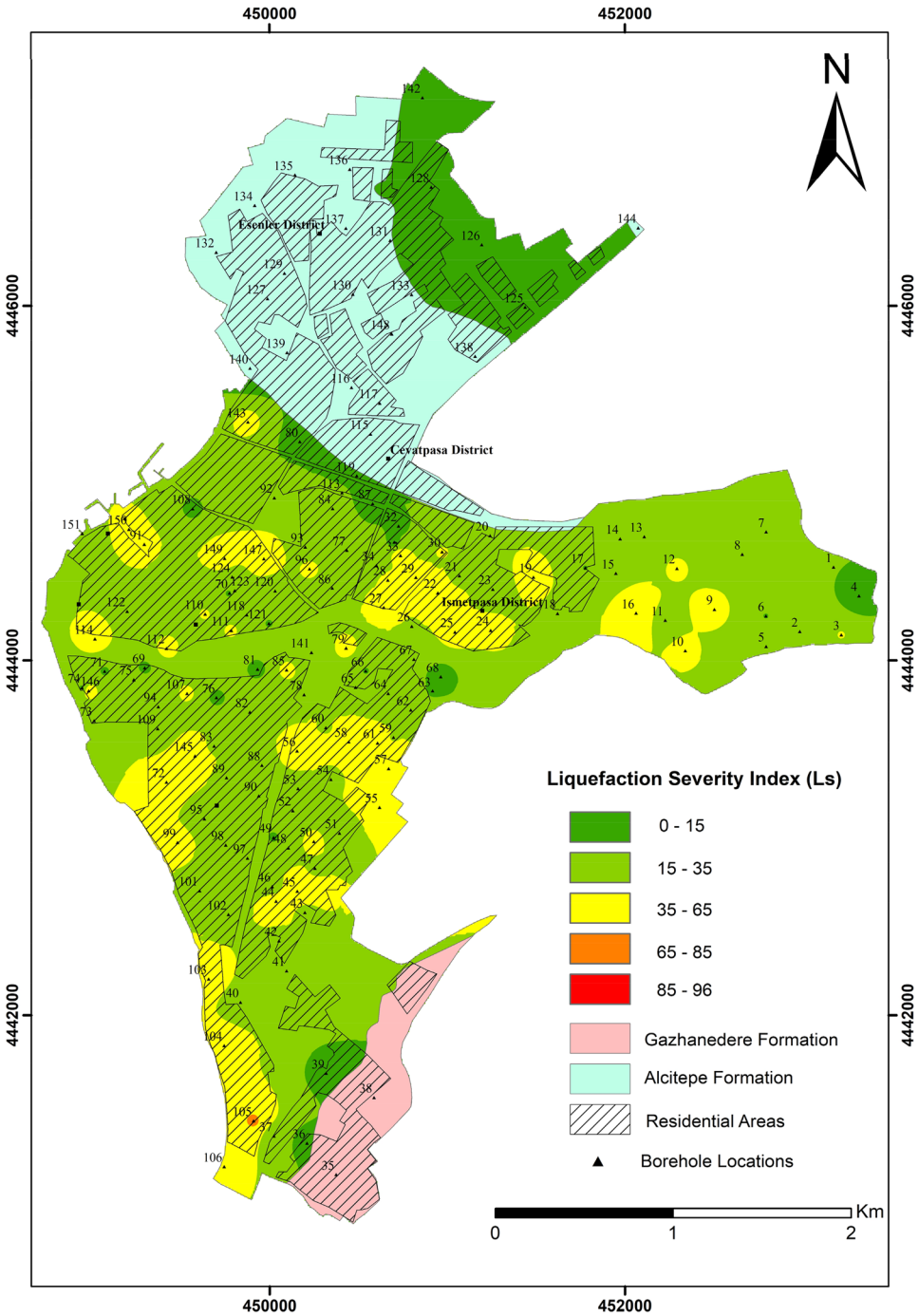

Fig. 14 Liquefaction severity map (a_{max} = 141 gal)

Thus, it is considered that the liquefaction severity index is more reliable than the liquefaction potential index.

5. In the study area, the Gazhanedere and Alcitepe Formations consist of sandstone and mudstone. Therefore, these formations were accepted as non-liquefiable soil.

The results of this study and liquefaction susceptibility maps can be used for urban-regional planning and risk management practices in Canakkale. In addition, the geotechnical properties of the liquefiable soils must be considered for proper foundation design of buildings in the Canakkale settlement area.

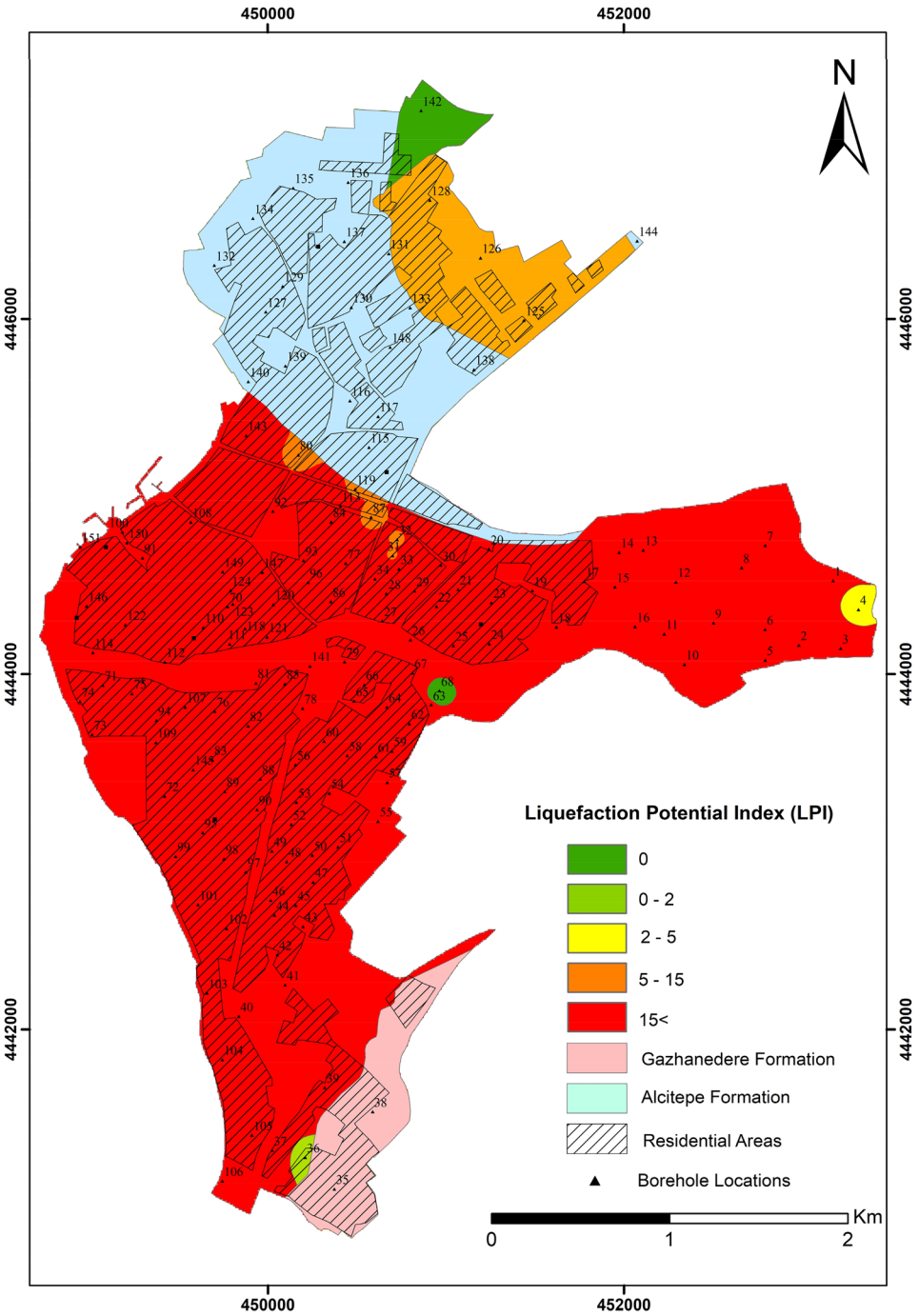

Fig. 15 Liquefaction potential map (a_{max} = 319 gal)

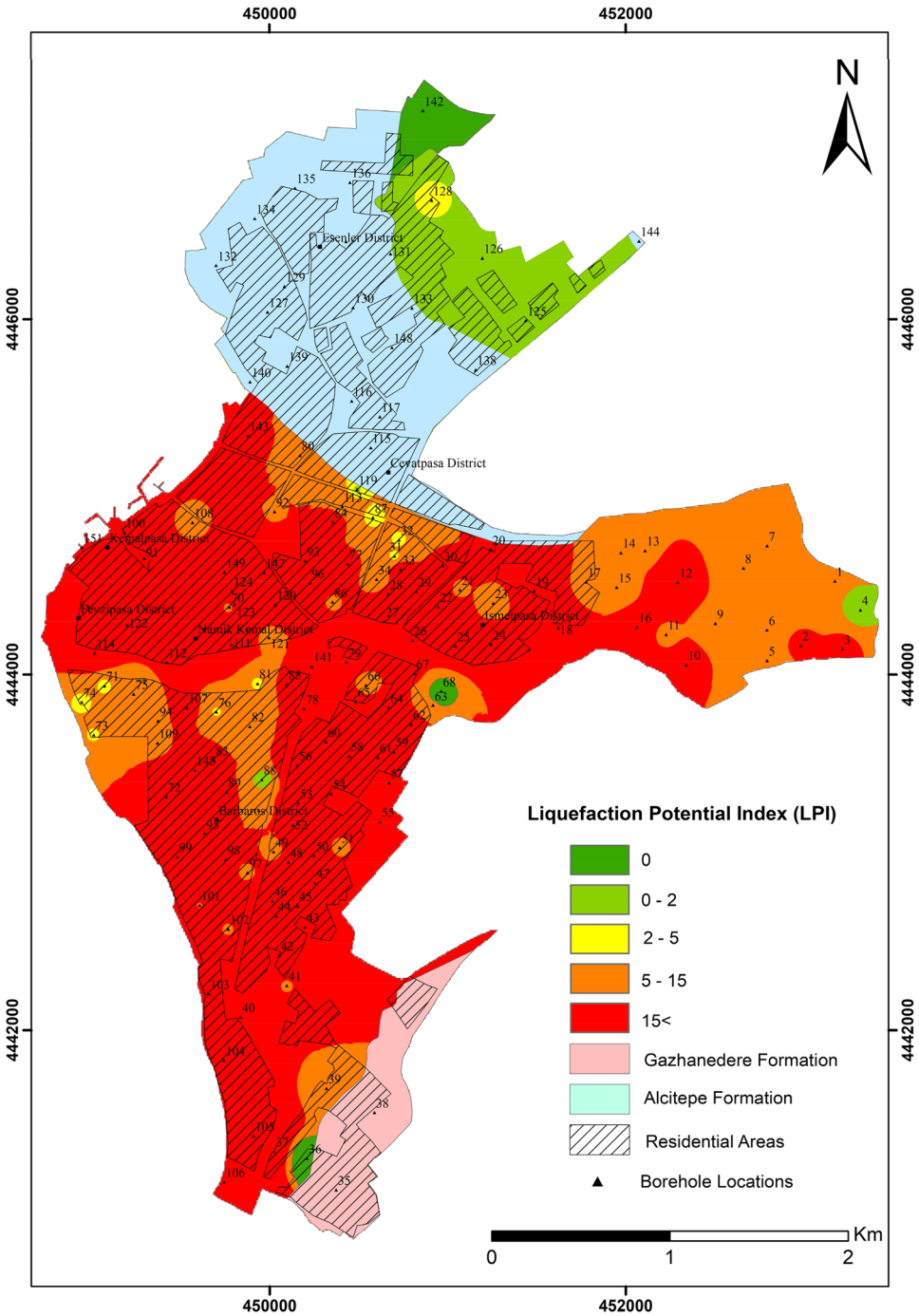

Fig. 16 Liquefaction potential map (a_{max} = 222 gal)

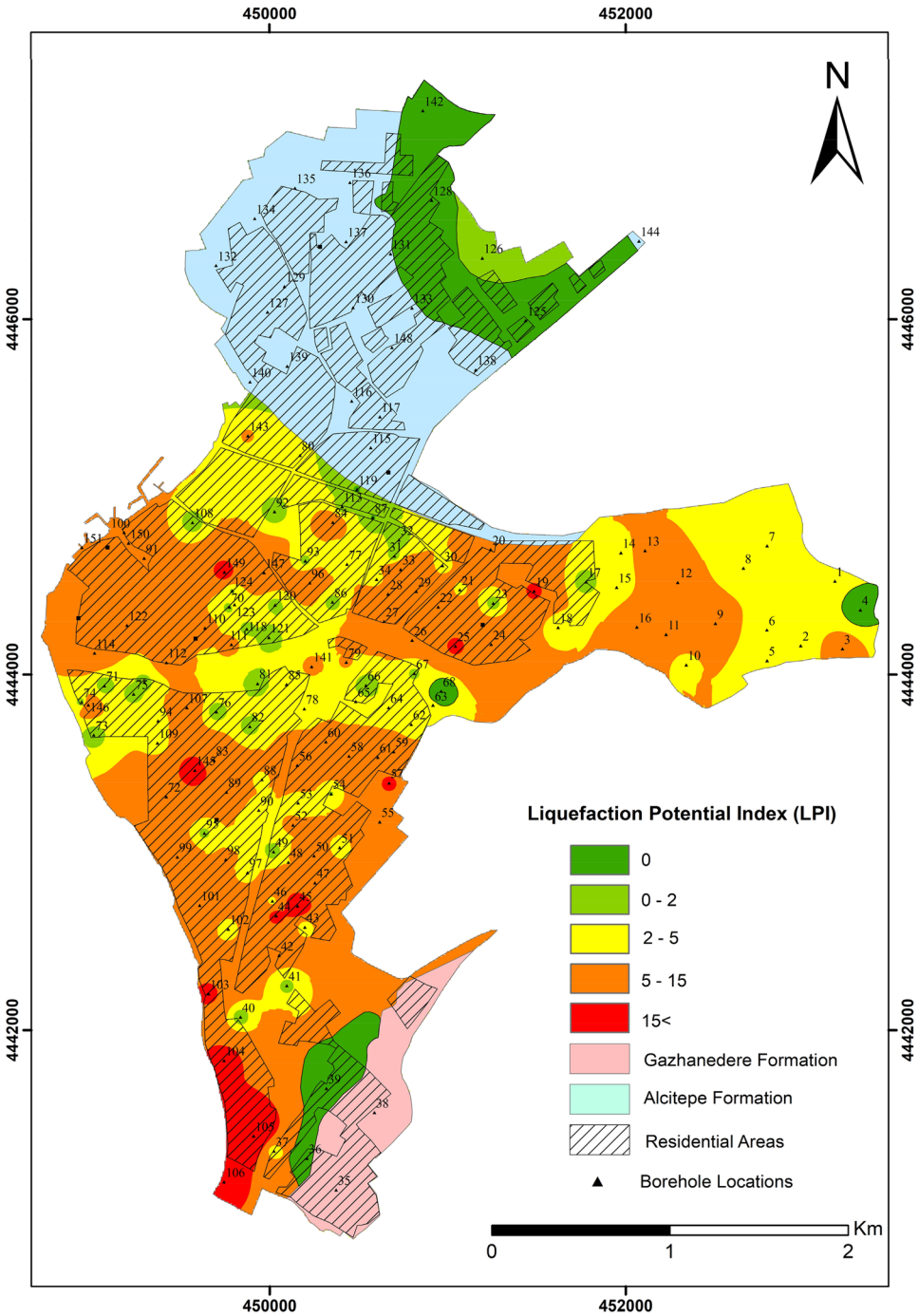

Fig. 17 Liquefaction potential map (a_{max} = 141 gal)

Acknowledgements The authors would like to express their gratitude to the municipality of Çanakkale for information and the logs of geotechnical boreholes. The authors also thank Saziye Ozge Dinc Gogus for valuable contributions during site investigations.

References

AFAD (Republic of Turkey Prime Ministry Disaster and Emergency Management Presidency) (2014) Earthquake Reports. http://kyhdata.deprem.gov.tr/2K/kyhdata_v4.php. Accessed 15 Jan 2018

AFAD (Republic of Turkey Prime Ministry Disaster and Emergency Management Presidency). http://www.deprem.gov.tr/en/eventcatalogue

Akin M, Ozvan A, Akin MK, Topal T (2013) Evaluation of liquefaction in Karasu River floodplain after the October 23, 2011, Van (Turkey) earthquake. Nat Hazards 69:1551–1575

American Society for Testing Materials (ASTM) (2004) Annual book of ASTM. standards-soil and rock, building stones, Section-4, Vol 04.08, p 1369

Atabey E, Ilgar A, Sakıtaş A (2004) Middle-Upper Miocene stratigraphy of Çanakkale, Çanakkale, NW Turkey. Bull Min Res Exp 128:79–97 **(in Turkish)**

Basaran-Uysal A, Sezen F, Ozden S, Karaca O (2014) Classification of residential areas according to physical vulnerability to natural hazards: a case study of Çanakkale, Turkey. Disasters 38(1):202–226

Buyuksarac A, Tunusluoglu MC, Bekler T, Yalciner CC, Karaca O, Ekinci YL, Alper D, Dinc SO (2013) Geological and geotechnical investigation project report of Canakkale settlement area prepared for Canakkale Municipality, p 234 (**in Turkish**)

Cetin KO, Seed RB, Der Kiureghian A, Tokimatsu K, Harder LF, Kayen RE, Moss RES (2004) Standard penetration test-based probabilistic and deterministic assessment of seismic soil liquefaction potential. J Geotech Geoenviron Eng ASCE 130(12):1314–1340

Chu BL, Hsu SC, Chang YM (2004) Ground behavior and liquefaction analyses in central Taiwan-Wufeng. Eng Geol 71:119–139

Deniz O (2005) Groundwater quality investigation of Canakkale settlement area. Canakkale Onsekiz Mart University, MSc Thesis, Graduate School of Natural and Applied Sciences, p 100 **(in Turkish)**

Dixit J, Dewaikar DM, Jangid RS (2012) Assessment of liquefaction potential index for Mumbai city. Nat Hazards Earth Syst Sci 12:2759–2768

Duman ES, İkizler SB, Angin Z (2015) Evaluation of soil liquefaction potential index based on SPT data in the Erzincan, Eastern Turkey. Arab J Geosci 8:5269–5283

General Directorate of Disaster Affairs (1996) The seismic zoning map of Turkey

General Directorate of Mineral Research and Exploration (MTA) (2012) Active fault map of Turkey

Gurbuz C, Aktar M, Eyidogan H, Cisternas A, Haessler H, Barka A, Ergin M, Turkelli N, Polat O, Ucer SB, Kuleli S, Baris S, Kaypak B, Bekler T, Zor E, Bicmen F, Yoruk A (2000) The seismotectonics of the Marmara region (Turkey): results from a microseismic experiment. Tectonophysics 316:1–17

Hasancebi N, Ulusay R (2006) Evaluation of site amplification and site period using different methods for an earthquake-prone settlement in Western Turkey. Eng Geol 87:85–104

Idriss IM, Boulanger RW (2004) Semi empirical procedures for evaluating liquefaction potential during earthquakes. In: Proceedings of the 11th international conference on soil dynamics and earthquake engineering and 3rd international conference on earthquake geotechnical engineering I, pp 32–56

Iwasaki T, Tokida K, Tatsuoka F, Watanabe S, Yasuda S, Sato H (1982) Microzonation for soil liquefaction potential using simplified methods. In: Proceedings of the 3rd international conference on Microzonation, Seattle 3, pp 1319–1330

Juang CH, Yuan H, Lee DH, Lin PS (2003) A simplified CPT-based method for evaluating liquefaction potential of soils. J Geotech Geoenviron Eng 129(1):66–80

Kang GC, Chung JW, Rogers JD (2014) Re-calibrating the thresholds for the classification of liquefaction potential index based on the 2004 Niigata-ken Chuetsu earthquake. Eng Geol 169:30–40

KOERI (Kandilli Observatory and Earthquake Research Institute) (2014) The Aegean Sea Earthquake on 24 May 2014 (Press Release)

Kramer SL (1996) Geotechnical earthquake engineering. Prentice Hall, Upper Saddle River, p 653

Lee DH, Ku CS, Yuan H (2004) A study of the liquefaction risk potential at Yuanlin, Taiwan. Eng Geol 71:97–117

Liao SSC, Whitman RV (1986) Overburden correction factors for SPT in sand. J Geotech Eng Div ASCE 112(3):373–377

Okay AI, Kaslılar-Ozcan A, Imren C, Boztepe-Guney A, Demirbag E, Kuscu E I (2000) Active faults and evolving strike-slip basins in the Marmara Sea, northwest Turkey: a multichannel seismic reflection study. Tectonophysics 321:189–218

Rahman MZ, Siddiqua S, Kamal ASMM. (2014) Liquefaction hazard mapping by liquefaction potential index for Dhaka City. Bangladesh Eng Geol 188:137–147

Rockwell T, Barka A, Dawson T, Akyuz S, Thorup K (2001) Paleoseismology of the Gazikoy-Saros segment of the North Anatolia fault, northwestern Turkey: comparison of the historical and paleoseismic records, implications of regional seismic hazard, and models of earthquake recurrence. J Seismol 5:433–448

Seed HB, Idriss IM (1971) Simplified procedure for evaluating soil liquefaction potential. J Soil Mech Found Div ASCE 107(SM9):1249–1274

Seed HB, Idriss IM (1982) Ground motions and soil liquefaction during earthquakes. Earthquake Engineering Research Institute, Berkeley, p 134

Seed HB, Tokimatsu K, Harder LF, Chung RM (1985) Influence of SPT procedures in soil liquefaction resistance evaluations. J Geotech Eng 111(12):1425–1445

Seed RB, Cetin KO, Moss RES, Kammerer AM, Wu J, Pestana JM, Riemer MF, Sancio RB, Bray JD, Kayen RE, Faris A (2003) Recent advances in soil liquefaction engineering: a unified and consistent framework. EERC Report No. 2003-06

Senturk K, Karakose C (1987) Geology of Canakkale Strait and surrounding. General Directorate of Mineral Research and Explorations. Archive of Geological Survey Department, unpublished technical report, 371, p 207 **(in Turkish)**

Sharma B, Hazarika PJ (2013) Assessment of liquefaction potential of Guwahati City: a case study. Geotech Geol Eng 31:1437–1452

Siyako M (2006) Thracian Basin Tertiary rock units. Stratigraphy Committee Lithostratigraphic Units Series-2, pp 43–83 **(in Turkish)**

Sonmez H (2003) Modification to the liquefaction potential index and liquefaction susceptibility mapping for a liquefaction-prone area (Inegol-Turkey). Environ Geol 44(7):862–871

Sonmez H, Gokceoglu C (2005) A liquefaction severity index suggested for engineering practice. Environ Geol 48:81–91

Sonmez B, Ulusay R (2008) Liquefaction potential at Izmit Bay: comparison of predicted and observed soil liquefaction during the Kocaeli earthquake. Bull Eng Geol Environ 67:1–9

Sonmez B, Ulusay R, Sonmez H (2008) A study on the identification of liquefaction-induced failures on ground surface based on the data from the 1999 Kocaeli and Chi-Chi earthquakes. Eng Geol 97:112–125

Tosun H, Ulusay R (1997) Engineering geological characterization and evaluation of liquefaction susceptibility of foundation soils at a dam site, southwest Turkey. Environ Eng Geosci 3(3):389–409

Tosun H, Seyrek E, Orhan A, Savaş H, Türköz M (2011) Soil liquefaction potential in Eskişehir, NW Turkey. Nat Hazards Earth Syst Sci 11:1071–1082

Tunusluoglu MC (2014) Assessment of the instability mechanism of spillway with reference to an earthfill dam in the northwest Turkey. Arab J Geosci 7:407–418

Ulamis K, Kilic R (2008) Liquefaction potential of Quaternary alluvium in Bolu settlement area, Turkey. Environ Geol 55:1029–1038

Ulusay R, Kuru T (2004) 1998 Adana-Ceyhan (Turkey) earthquake and a preliminary microzonation based on liquefaction potential for Ceyhan town. Nat Hazards 32:59–88

Ulusay R, Aydan O, Kumsar H, Sonmez H (2000) Engineering geological characteristics of the 1998 Adana-Ceyhan earthquake, with particular emphasis on liquefaction phenomena and the role of soil behaviour. Bull Eng Geol Environ 59:99–118

Ulusay R, Tuncay E, Sonmez H, Gokceoglu C (2004) An attenuation relationship based on Turkish strong motion data and iso-acceleration map of Turkey. Eng Geol 74:265–291

Ulusay R, Tuncay E, Hasancebi N (2007) Liquefaction assessments by field-based methodologies: foundation soils at a dam site in Northeast Turkey. Bull Eng Geol Environ 66:361–375

Vipin KS, Sitharam TG, Anbazhagan P (2010) Probabilistic evaluation of seismic soil liquefaction potential base on SPT data. Nat Hazards 53:547–560

Well DL, Coppersmith KJ (1994) New empirical relationships among magnitude, rupture length, rupture width, rupture area, and surface displacement. Bull Seismol Soc Am 84(4):974–1002

Yalcin A, Gokceoglu C, Sonmez H (2008) Liquefaction severity map for Aksaray city center (Central Anatolia, Turkey). Nat Hazards Earth Syst Sci 8:641–649

Yaltırak C, Işler EB, Aksu AE, Hiscott AE RN (2012) Evolution of the Bababurnu Basin and shelf of the Biga Peninsula: Western extension of the middle strand of the North Anatolian Fault Zone, Northeast Aegean Sea, Turkey. J Asian Earth Sci 57:103–119

Yildirim A, Akdur O, Ozcelik H (2015) Injuries and emergency department visits without building destruction after Gökçeada earthquake in Çanakkale, Turkey. Notfall Rettungsmed 18:377–380

Yilmaz I, Bagci A (2006) Soil liquefaction susceptibility and hazard mapping in the residential area of Kütahya (Turkey). Environ Geol 49:708–719

Yilmaz I, Yavuzer D (2005) Liquefaction potential and susceptibility mapping in the city of Yalova, Turkey. Environ Geol 47:175–184

Youd TL, Idriss IM, Andrus RD, Arango I, Castro G, Christian JT, Dobry R, Finn WDL, Harder LF, Hynes ME, Ishihara K, Koester JP, Liao SSC, Marcuson WF III, Martin GR, Mitchell JK, Moriwaki Y, Power MS, Robertson PK, Seed RB, Stokoe IIKH. (2001) Liquefaction resistance of soils: summary report from the 1996 NCEER and 1998 NCEER/NSF workshops on evaluation of liquefaction resistance of soils. J Geotech Geoenviron Eng 127:817–833